A MONTE CARLO SIMULATION OF SURFACE KINETICS DURING PLASMA ENHANCED CHEMICAL VAPOR DEPOSITION OF SILICON DIOXIDE USING TETRAETHOXYSILANE CHEMISTRY

BY

PHILLIP J. STOUT

B.S., University of Illinois, 1989

THESIS

Submitted in partial fulfillment of the requirements
for the degree of Master of Science in Electrical Engineering
in the Graduate College of the
University of Illinois at Urbana-Champaign, 1991

Urbana, Illinois

UNIVERSITY OF ILLINOIS AT URBANA-CHAMPAIGN

THE GRADUATE COLLEGE

JULY 1991

WE HEREBY RECOMMEND THAT THE THESIS BY

PHILLIP J. STOUT

ENTITLED A MONTE CARLO SIMULATION OF SURFACE KINETICS DURING PLASMA ENHANCED CHEMICAL VAPOR DEPOSITION OF SILICON DIOXIDE USING TETRAETHOXYSILANE CHEMISTRY

BE ACCEPTED IN PARTIAL FULFILLMENT OF THE REQUIREMENTS FOR THE DEGREE OF MASTER OF SCIENCE

Mark J. Kushner
Director of Thesis Research

Timothy N. Kirk
Head of Department

Committee on Final Examination†

Chairperson

† Required for doctor's degree but not for master's.

O-517

TABLE OF CONTENTS PAGE

I. INTRODUCTION

The need for deposition of SiO_2 films (oxide) having good conformal qualities at low temperatures has motivated a renewed interest in tetraethoxysilane (TEOS, $Si(C_2H_5O)_4$) as a source gas in plasma enhanced chemical vapor deposition (PECVD). Oxide grown with TEOS has been shown to have good conformal qualities with acceptable or moderate insulating properties, even when deposited at low temperatures. This is important when considering some of the uses of the film. In interlayered dielectrics,[1] it is important to fill the submicron spacings without voids and in some cases form a planar surface.[2] In insulation between conductive multilevel layers in the metalization process,[3] a low temperature deposition is important which has good insulation properties and conformality. Depositions at a low temperature are important due to the stringent thermal budgets dictated by hillock or clump formation by Al contacts at temperatures above 450°C[4] and the presence of shallow junctions, which would diffuse more rapidly into the substrate at higher temperatures.

A competitor to TEOS SiO_2 film deposition using plasmas is the oxidation of silane (SiH_4). This process, however, suffers from poor insulating quality and very poor conformality.[5] In fact, poor conformality due to effects such as step coverage cusping is a well-known characteristic of SiH_4 based PECVD oxides and is thought to be due to the low surface mobility of adsorbed SiH_4 intermediates.[6] Considering these shortcomings, TEOS provides better film properties than those obtained with silane chemistry[7] mostly due to a higher surface mobility. In addition, TEOS is easier to handle and much safer than silane.[8] Understanding the kinetics of low temperature SiO_2 film deposition using TEOS + O_2 chemistry is therefore of some interest.

X-ray photoelectron spectroscopy (XPS) studies[9] have shown a low carbon content in oxide deposited using the PECVD process with TEOS/O_2 chemistry, which implies that the plasma dissociates most of the TEOS and oxygen to form reactive species prior to incorporation into the bulk film. Other work[10] suggests that the TEOS surface adsorption is accomplished through TEOS fragments, partially decomposed by plasma or radicals, impinging the surface. Partially decomposed TEOS species, because they have unsatisfied orbitals, can be chemisorbed on the substrate surface. These adsorbed TEOS species are eventually incorporated into the oxide and

have been hypothesized to have forms such as $(SiO)_2Si(OC_2H_5)_2$ and $(SiO)Si(OC_2H_5)_3$ from results of transmission infrared spectroscopy.[11] The extent of the surface reaction to create these species appears to be somewhat dependent on the surface OH concentration.

It has been observed that the deposition rate of PECVD oxide using TEOS/O_2 chemistry has a negative activation energy. The processes responsible for this observation are believed to be highly dependent on the generation of reactive radical species of TEOS in the plasma and the adsorption/desorption rate of the reactive TEOS radicals on the substrate surface.[12] The observed high conformality of the film compared to other PECVD systems implies that a TEOS radical once adsorbed onto the film should have a high degree of surface mobility.

In fact, isotopic labeling and step coverage studies of TEOS oxide deposition support a mechanism dominated by surface reactions.[13] In the past, analytical models have been developed[14,15] which stress events occurring in the plasma over reactions on the surface. Other models using a Monte Carlo Method and concerned with step coverage exist but are not specific to TEOS.[16,17] Therefore, a computer model using FORTRAN has been written to simulate PECVD of oxide (SiO_2) using TEOS/O_2 chemistry with particular emphasis placed on surface effects.

In the following sections the approach to modeling the deposition environment will be discussed with emphasis placed on the assumptions made concerning the plasma, the representation of the deposition surface or substrate, and the types of processes taking place in the substrate and on the substrate surface. The model is then used to analyze features of the oxide around a "canonical" case. The quantities to be investigated include growth rate, fraction of carbon and silanol, conformality, and roughness of the oxide.

II. DESCRIPTION OF THE MODEL

A. Plasma Kinetics

The radicals that will eventually form the deposited film on the substrate constituting the oxide are generated in the plasma. In thermal CVD the energy to dissociate the TEOS into radicals comes from the heated substrate. On the other hand, PECVD uses an rf or in some cases a microwave discharge to dissociate and oxidize TEOS + O_2 into the chemical precursors needed for the oxide deposition. The result is that the substrate temperatures can be lower than those needed for thermal CVD.

In general, a typical plasma is defined in terms of the rf frequency and power, pressure, the O_2/TEOS ratio, and their respective flow rates. Typical conditions are a 13.56 MHz rf discharge running at hundreds of watts, a plasma pressure of 1 Torr with an O_2/TEOS ratio of 0.5 to 50 with TEOS flow rates of 25 standard cm^3/min (sccm) and a parallel plate reactor with electrodes separated by 1.3 cm and measuring approximately 31.1 cm in diameter. These parameters may change depending on whether a microwave plasma is being considered instead of an rf plasma, whether the plasma is remote or not, and so on.

The chemical formula for TEOS is $Si(C_2H_5O)_4$ abbreviated here as SiX_4 where the X "group" is equivalent to C_2H_5O. The two types of reactions hypothesized to take place in the plasma which generate deposition precursors are electron impact

$$\begin{aligned} e + SiX_4 &\rightarrow SiX_3(OH) + C_2H_4(g) + e \\ e + SiX_3(OH) &\rightarrow SiX_2(OH)_2 + C_2H_4(g) + e \\ e + SiX_2(OH)_2 &\rightarrow SiX(OH)_3 + C_2H_4(g) + e \\ e + SiX(OH)_3 &\rightarrow Si(OH)_4 + C_2H_4(g) + e \\ e + O_2 &\rightarrow O + O + e \end{aligned} \qquad (1)$$

and O insertion

$$\begin{aligned} O + SiX_4 &\rightarrow SiX_3(OH) + C_2H_4O(g) \\ O + SiX_3(OH) &\rightarrow SiX_2(OH)_2 + C_2H_4O(g) \\ O + SiX_2(OH)_2 &\rightarrow SiX(OH)_3 + C_2H_4O(g) \\ O + SiX(OH)_3 &\rightarrow Si(OH)_4 + C_2H_4O(g) \end{aligned} \qquad (2)$$

In both reaction types an X group is removed from the silicon complex and is replaced by an OH group. Electron impact processes are dissociating the O_2 as well.

The O insertion reactions are the most important set of reactions when dissociating TEOS[18] as well as the removal of X groups from the film. The importance of O insertion can be rationalized in part by the fact that most TEOS plasmas operate highly diluted by O_2 (O_2/TEOS $\approx$ 95/5); therefore, most of the energy deposited in the plasma goes into the O_2. In some cases deposition is done with remote plasmas which do not even have the TEOS in the discharge where the hot electrons are likely to be. In general, the plasma is primarily dissociating O_2 through electron impact reactions, and the resulting O radicals react with the TEOS, removing C_2H_4O. These radicals are created in such a way that the deposition surface or substrate can be held at significantly lower temperatures than for a thermal CVD process.

There are other reactions occurring in the plasma, but the major concern in this study is the surface kinetics of the deposition process. In this model one simply specifies the flux of radicals to the surface consistent with the cited reaction scheme. One can have five types of gas phase radicals, $Si(OH)_4$, $SiX(OH)_3$, $SiX_2(OH)_3$, $SiX_3(OH)$, and O. The relative concentrations and the total flux of these are determined mainly by the power deposited into the plasma. The plasma parameters are chosen so that the most important process in the temperature range of interest is plasma generated radicals bombarding the film, as opposed to thermal decomposition. SiX_4 is not considered since there is no mechanism for it to be integrated into the film at low substrate temperatures.

B. Substrate

1. Sites

The basis of this model, as shown in Figure II-1, is to treat the substrate as a collection of sites held in a three-dimensional array with each site denoting the status of a silicon complex. The sites are held in stacks or columns and their level in the stack determines the type of site. The first *depth* number of sites from the surface are referred to as near sites. Any site deeper into the stack is called a buried site. The *depth* of the surface of the oxide is user defined.

a. Near sites

A near site distinguishes itself from other types in that it is located close to the surface of the oxide, carries bond information on a Si complex, and holds a unique position. When a radical

is integrated into the film, the site is identified by the type of bonds the silicon associated with that site engages in. Silicon has four possible bonds and, given the chemical composition of the incident plasma radicals assumed by the model, can bond to one of three specis. It can bond to an O atom in the SiO_2 network, to an OH group, or to an X group. No attempt is made in tracking the directionality of each particular bond. Given these assumptions and the fact that one of the bonds has to be to the amorphous SiO_2 network, there are eleven possible types of sites as noted in Figure II-1. The nomenclature is B denotes bonding of Si to oxygen, X denotes Si bonding to C_2H_5O, O denotes Si bonding to OH. Voids are also included.

A near site is then the mainstay of the substrate and carries the most exacting information. A void is also included as a near site since it is actually keeping track of the absence of a Si complex in the amorphous SiO_2 network, as discussed below.

b. Voids

If there is a gap in the amorphous SiO_2 network (i.e., no Si complex) then it is referred to as a void. A void is formed when two silicon sites interlink (defined later) a site away from each other instead of to an adjacent type. The site between them through which the bonds extend is referred to as the void. The bonds above the gap which create the void are assumed to block any radicals which may want to integrate into the film below it. When the bond forms, all open sites below it become voids as well. Since there are no processes which can change the status of a void, once the void forms it becomes a permanent fixture of the film.

c. Buried sites

Given computer memory and speed considerations, every site within the wafer can not be kept track of. The solution is to keep track of only a finite number of sites. As a site gets buried deeper into the film or moves farther down in the stack of sites, it is considered to become more a property of the wafer and less of the surface. The model treats this deeply embedded site as a bulk statistic or buried site. That is, the site type is averaged to track the number and type of atoms entering the bulk film. Each stack has only a *depth* number of layers which have full statistics, with the height of the stack determined by the number of buried sites under this near layer. Thus as radicals adsorb onto the surface and incorporate into the film becoming near sites piled on a stack,

near sites under it are moving deeper into the stack. Eventually, if a near site becomes greater than *depth* deep in the stack, it is buried and becomes "statistical". It is called a buried site in the sense that it was formerly a near site but has since fallen off the bottom of the stack.

The assumptions have repercussions on processes such as interlinking defined in the next section wherein a site which is rapidly buried (defining a small depth layer) may not have sufficient time to eliminate its extra hydroxyl groups. In addition, sites attempting to bond to a location that has been buried cannot rid themselves of hydroxyl groups.

2. Reactions

The primary reaction that takes place in the substrate is an interlinking step

$$\text{Si-OH} + \text{OH-Si} \rightarrow \text{Si-O-Si} + \text{H}_2\text{O} \tag{3}$$

where the hydroxyl (OH) groups of adjacent silicon complexes in the film react to eliminate water, and two silicon atoms bond to a shared oxygen. This reaction also occurs on the surface allowing radicals not yet part of the film to integrate into the film. In addition the reverse reaction gives a mechanism for water to integrate into the film in the form of OH groups.

The other reaction considered is pyrolysis

$$\text{Si-X} \rightarrow \text{OH-Si} + \text{C}_2\text{H}_4(\text{g}) \tag{4}$$

where an X group of a Si complex becomes a hydroxyl group with the release of C_2H_4. The source of energy for this reaction comes from the heat of the substrate. Since TEOS pyrolyzes at about 700°C, this reaction plays a small part in the PECVD of oxide but plays an integral part in the thermal CVD of oxide.

The possibility of O_2 in the plasma reacting directly with the Si to form SiO_2 has been shown to be very unlikely to occur at the substrate temperatures of interest.[13]

3. Surface before deposition

The substrate is assumed to be initially passivated such that the sites on the top layer are almost completely integrated into the film, having three of their bonds connected to an O atom of the film with only the last connected to an OH group pointing up. More concisely, the top layer before growth consists of BBBO sites.

Under the BBBO surface layer is *depth - 1* layers of pure SiO_2 denoted in the model as BBBB sites. Thus, even as the first radicals fall to the substrate and integrates into the film, BBBB sites are being buried. The substrate is initially smooth but the model can simulate deposition on rougher surfaces. Also the initial surface site types are not limited to BBBO sites but can be a mixture of those shown in Figure II-1.

C. Timed Processes

There are four surface processes and three bulk processes in the model schematically shown in Figure II-2. The surface processes are radicals adsorbing onto the surface, radicals moving from site to site, radicals desorbing from the substrate, and O radicals bombarding the substrate. The bulk processes are interlinking or densification of the film, void formation, and pyrolysis.

These processes are not the only ones in the model, but they are the ones that have a specific rate associated with them. These processes have rates, or mean times of occurrence Δt, associated with them because the speed of their occurrence affects other processes. An example of an event without a Δt is the integration of the radical into the film, which is essential to film growth, but does not have a defined rate in the model. A way of rationalizing the omission is that the amount of time taken to bond the radical to the oxide will not affect the other processes. If new radicals landing on a bond in progress cause some effect, the bonding process could be timed. No such occurrences are included in this model so the bonding process does not have a completion time associated with it.

All of the processes having rates are related to the substrate temperature. The parameterization of the various processes as a function of substrate temperature and comparing to experimental results provides validation of the model. It should be noted that all of the following temperature dependencies are only valid in the PECVD temperature regime (approximately 350 - 425°C) and become invalid if other temperatures are used.

A flow chart of the model shown in Figure II-3 shows the timed processes in the model. Also included in the flow chart are the radical processes covered in the next section.

1. Radical adsorption

A radical from the plasma adsorbs onto the substrate surface every Δt_{ads} seconds. Given the operational temperatures of a PECVD reactor, radical adsorption is independent of the substrate temperature and essentially dependent on the physics and conditions of the plasma. That is, the energy to dissociate TEOS is coming from an rf discharge and not from the thermal energy of the substrate. Therefore, increasing the substrate temperature should have no effect on the number of radicals incident on the surface.

The time between radicals adsorbing onto the surface is usually calculated from an input radical flux represented by Φ_{rad} ($cm^{-2}s^{-1}$) . Therefore,

$$\Delta t_{ads} = \frac{10^{16}}{3.5^2 \cdot x \cdot y \cdot \Phi_{rad}} s \tag{5}$$

where 3.5 Å is the average size of a site, 10^{16} is a conversion factor from $Å^2$ to cm^2, x and y are the dimensions of the computational substrate in units of number of sites, and Φ_{rad} is the user-defined flux.

The radical flux Φ_{rad} plays a major role in the growth rate since increasing the flux of incident radicals allows more chances for a radical to integrate into the surface per unit time. More precisely it sets a maximum growth rate if all of the radicals instantly become part of the film. Consider a 10 x 10 film in which 10 layers have to be deposited. If the film is assumed to be perfectly smooth, a total of 1000 sites need to be "filled". Bringing these 1000 sites to the surface takes a finite amount of time so the maximum growth rate is limited by the rate at which new sites reach the substrate. The maximum growth rate is $1/[(\Delta t_{ads})(10 \times 10)]$ in layers per second or the reciprocal of the time needed to grow a layer.

2. Radical movement

The radical movement increment is the time required to move from one site to the next. It is usually the most rapid of the five processes and thus becomes the basic increment of time used when the global clock is moved forward. The temperature dependence is resolved when considering that once a radical has adsorbed onto the surface and is caught in the potential well

formed by the surface sites, it has a certain probability of moving from one potential well to another which increases with temperature. One then assumes

$$\Delta t_{mov} = 6x10^{-7}\exp\left[\frac{\Delta E}{RT}\right] s \quad (6)$$

where the activation energy ΔE=1900 J/mole, R is the molar gas constant which is 8.31441 J/mole·K, and T is temperature in Kelvin . A faster moving radical is associated with higher temperatures. Figure II-4 shows a plot of the above function.

3. Radical residence time on surface

The radical is allowed a certain maximum amount of time Δt_{res} on the surface to attempt to integrate into the film. If in this increment of time it fails to integrate into the film it desorbs from the surface of the growing oxide. A radical can integrate into the film in a shorter amount of time, the residence time Δt_{res} is only the maximum amount of time.

The residence time of the radical on the surface becomes intertwined with the first two processes affecting the mobility (or number of possible sites visited) of the radical as well as the number of radicals on the surface. Increasing the residence time on the surface gives a radical a broader area of movement which in turn lets a radical incorporate into the film at a point farther away from where it landed. This increases its effective mobility since more move intervals can fit into a Δt_{res}. Alternatively, an increase in mobility is caused by decreasing the move time and keeping the residence time fixed. The other effect involves the time between radicals arriving on the surface. If Δt_{ads} is made less than a radical's maximum surface time, more than one radical could be present on the computational surface. Alternatively, a Δt_{ads} which is larger than Δt_{res} insures that only one radical is on the surface at any one time.

The radical's surface residence time dependence on temperature has been shown to have an associated activation energy.[19] It is theorized in this model that

$$\Delta t_{res} = 3x10^{-5}\exp\left[\frac{\Delta E}{RT}\right] s \quad (7)$$

where ΔE= 21800 J/mole. A plot of the temperature dependence is shown in Figure II-5. The equation suggests that as temperature increases the total time the radical could possibly spend on

the surface decreases. Given the observed negative activation energies for the PECVD of oxide using TEOS, this is an important effect.[20]

4. Interlinking or densification

The interlinking reaction is

$$\text{Si-OH} + \text{OH-Si} \rightarrow \text{Si-O-Si} + H_2O \qquad (8)$$

as noted earlier. That is, two adjacent sites of the same height are checked to see if they have an OH group to contribute to the reaction. If they do, then the reaction occurs and the site types are changed to reflect the occurrence. A subtlety in implementation, however, makes it a little more complicated. If all of the surface sites are allowed to interlink with nearest neighbors, all of the OH surface sites would be used up in the reactions. The result would be no OH groups for incoming radicals to react with on the surface and integrate into the film. The film would then effectively halt its growth. When interlink is implemented, the surface sites are always left with an OH group (with the exception of BXXX). This always insures available bonds to keep the growth of the film in an upward direction and requires most sites to have one bond straight up.

Interlinking is a very important process since it rids the oxide of the extra silanol in the film and the electrical properties of deposited oxides are strongly influenced by the amount of hydrogenated species present in the film.[21] In fact, as higher concentrations of water and silanol (SiOH) are incorporated into the film, the stability and electrical properties of the deposited oxide film are increasingly degraded.[22] Low temperature oxide has to meet all the criteria for submicron device applications. These criteria include low silanol (SiOH) and water content (as well as low film stress, high electrical resistivity, and minimum proton content).[23] Indeed low silanol content is an attribute of *good* film.

The interlinking should be occurring at a continuous rate, but in this model, the whole wafer is checked for possible interlinkages every Δt_{int} interval of time. Interlinking frequency becomes important when considering the amount of OH being left in the film. If the interlink is not fast enough, the site could be buried before it loses the extra silanol through bonding with an adjacent site having an OH group.

Densification's dependence on temperature is minimal in the PECVD temperature regime. Films are usually densified by ions from the plasma bombarding the film and imparting to it the energy needed to undergo densification, or after PECVD, through rapid thermal anneal (RTA).

5. Void formation

Voids are formed following the same general rules as interlinking but, as shown in Figure II-6, instead of bonding between nearest neighbors bonding occurs between next nearest neighbors. There is the additional restriction that there be no site between them (near, buried, or void) before the bond occurs. The time between void formation, or attempted void formation, is independent of interlinking, though it is assumed to be a much slower process ($\Delta t_{voi} >> \Delta t_{int}$). Void as used here does not refer to the huge void that could possibly form when trying to completely fill a trench but rather pinholes in the film. In the case of TEOS chemistry, few voids or pinholes have been found making this effect less prominent.

6. Oxygen radicals incident on the substrate

An O radical is incident on the substrate every Δt_o "click" of the global clock. That is, an O radical hits a surface site picked at random (subject to the global geometric shadowing if a trench is considered). If the site has an X group, an O insertion reaction is assumed to take place. The result is a replacement of one of the silicon atom's X bonding partners to an OH group.

This is one of the two processes considered in reducing the carbon (or X group) content of the film. In general, X group removal becomes important when a large majority of adsorbing radicals have three X groups. If there were no process to remove the X groups, the film growth could be halted if the top layer is all BXXX groups. Also, experimental data show low carbon content in the film except for the surface[9] and mechanisms are needed to reduce carbon content given that the radicals coming to the surface contain carbon. The substrate temperature has no effect on the O flux impinging on the surface since the supply of O is coming from the plasma.

The time between O radicals incident on the surface is usually calculated from an input flux represented by Φ_{oxy} ($cm^{-2} \cdot s^{-1}$). Therefore,

$$\Delta t_o = \frac{10^{16}}{3.5^2 \cdot x \cdot y \cdot \Phi_{oxy}} s \qquad (9)$$

where 3.5 Å is the average size of a silicon complex, 10^{16} is a conversion factor from $Å^2$ to cm^2, x and y are the dimensions of the computational substrate in units of number of sites, and Φ_{oxy} is the user-defined flux.

7. Pyrolysis

Pyrolysis causes an X group to change to an OH group every Δt_{pyr} tick of the global clock

$$\text{Si-X} \rightarrow \text{OH-Si} + C_2H_4(g). \tag{10}$$

The model randomly chooses a site in the near layer and changes an X group to an OH group if the site has any X groups. This is different from O radical impingement in that the reaction can occur in the near layer as well as on the surface. Also pyrolysis is driven by high substrate temperatures whereas O radical impingement has no dependence on substrate temperature.

The fact that a high substrate temperature is needed before this process begins to dominate can be seen in the high activation energy for the process. It is asserted in the model that

$$\Delta t_{pyr} = 5x10^{-14}\exp\left[\frac{\Delta E}{RT}\right] s \tag{11}$$

where the activation energy ΔE= 184096 J/mole. A plot of Equation (11) is shown in Figure II-7 demonstrating the high temperatures needed for this process to be important. The plot shows smaller Δt_{pyr} as temperature is increased. As mentioned earlier, this process plays little part in the PECVD of oxide but does becomes a dominate process when substrate temperature is increased to the levels of a thermal CVD process (600°C - 800°C)

8. Global clock

The global clock "ticks" away the simulated time of the deposition and is the method used to keep track of the last occurrence of a process and to determine the order of occurrence of the timed processes. Each process's Δt is added to its respective last recorded occurrence time to get the process's time of occurrence in the future. In any given loop in the model, all the processes are implemented which have their occurrence time less than or equal to the current global clock time (i.e., $t_{\text{last occurrence}} + \Delta t_{process} \leq t_{global}$). The processes which occur have their occurrence time updated using the current global clock time and their respective Δt's.

The global clock is incremented by the Δt of the fastest process (i.e., $\Delta t=\min\{\Delta t_{ads}, \Delta t_{mov}, \Delta t_{res}, \Delta t_{int}, \Delta t_{voi}, \Delta t_{o}, \Delta t_{pyr}\}$). This insures that during each loop of the model the fastest process will always occur. Also, other processes are insured never to be skipped over or at least to occur at their future occurrence times plus or minus the fastest process increment of time ($\pm\Delta t$).

It should be noted however that moving the clock forward the minimum Δt may not always insure a process occurring. If all the radicals have integrated into the film or have desorbed, then ticking the global clock forward to the next radical move time (usually the fastest process) will accomplish nothing. That is, the only thing that is supposed to happen is to move non-existent radicals around on the surface. If no radicals are on the surface of the substrate, the clock is speeded up to the time the next earliest process is set to occur.

D. Radical Processes

A PECVD plasma with 95/5 O_2/TEOS creates many radicals, of which $Si(OH)_4$, $SiX(OH)_3$, $SiX_2(OH)_2$, $SiX_3(OH)$, and O_2 are allowed to collide with the surface.

As noted earlier, it is possible to choose process parameters such that more than one radical is simultaneously on the surface. However, this model makes no account of radical-radical interactions. The result is that they are oblivious to each other and can occupy the same site on the wafer or pass through each other when being moved around on the surface, for instance, if two radicals occupy the same spot and one successfully bonds. All the other radical can sense is that the stack is being elevated by one site. Items that are considered in the model are reaction probability, geometric shadowing, radical movement, and barriers on the substrate surface.

1. Reaction probability

When both a radical and a substrate site have an OH group to contribute to an integration reaction, it does not automatically occur. A bond resulting from a surface reaction occurs only with probability P_r. A radical adsorbed on the surface diffuses from site to site and when it encounters an OH on the surface to react with, a random number is selected and compared with P_r. If the random number is less than or equal to P_r, the reaction is allowed to occur; otherwise, the reaction is not allowed and the radical moves on. This surface reaction probability P_r plays a part in the effective mobility of the radical on the surface since the ratio of $\Delta t_{rcs}/\Delta t_{mov}$ determines only the

potential maximum number of moves on the surface while P_r controls the actual number of sites visited.

The reaction probability has a certain activation energy or a dependence on temperature given by

$$P_r = 0.0005\exp\left[\frac{\Delta E}{RT}\right] \tag{12}$$

where the activation energy ΔE=-2061 J/mole. On perusal, one sees an increase in the bonding probability as temperature increases, although due to the low activation energy, the reaction probability varies little in the PECVD temperature regime (approx 350 to 425°C). A plot of P_r is shown in Figure II-8.

The gradual change of P_r in the PECVD temperature range is needed when considering the negative activation energy observed for the growth rate of PECVD of oxide using TEOS chemistry and the sensitivity of P_r to the growth rate. A negative activation energy implies a decrease in the growth rate of the film as temperature is increased whereas an increase in P_r with temperature causes increased growth rates. The reaction probability is a process opposing the decrease of growth rate for increased temperatures; if its variation with temperature is made small, other effects will dominate and provide the desired growth rate dependence on temperature.

The gradual change in P_r with temperature, required to explain the negative activation energy, can be determined from the effective probability that a radical is incorporated into the film;

$$P_i = 1-(1-P_r)^{\Delta t_{res}/\Delta t_{mov}}. \tag{13}$$

The larger P_i is, the higher is the growth rate.

This expression is plotted in Figure II-9 for two different residence times and shows an increase in the incorporation probability P_i as the bonding probability increases. As temperature increases, however, the ratio $\Delta t_{res}/\Delta t_{mov}$ increases/decreases. The time on the surface decreases with increasing T more quickly than the interval between moves, causing the exponent to decrease as temperature increases. Since (1-Pr) < 1 and $\Delta t_{res}/\Delta t_{mov}$ decreases as T increases, the incorporation probability goes down if P_r varies little. If P_r were to change drastically with temperature, however, it could outweigh the exponential change and a positive activation energy

for the growth rate would result. Thus a small variation of P_r in the PECVD range of temperatures is needed to maintain a negative activation energy for growth.

2.Geometric shadowing

a. Local

When a radical is incident on the surface, an accounting is made for the isotropic nature of incoming radicals. If one were to supply a randomly chosen position for radical absorption, no accounting would be made for the physical surroundings of the site. This approach is valid if the radicals are arriving normal to the substrate surface, that is, purely anisotropic. If the incoming radicals do not strike the substrate with normal incidence, however, a stack in the wafer could be shadowed by a stack next to it. This is accounted for in the model as shown in Figure II-10. First, an initial landing site for the radical is randomly chosen. The differences in the heights of the eight stacks surrounding the landing site to the stack initially selected as the landing site are then calculated. Any negative height differences are ignored and the resulting values are used to obtain the average shadowing height. The acceptance angle of a site next to two stacks of average shadowing height is then used to get the probability that an incident radical lands on the initially selected stack and is not shadowed by a surrounding stack. If that site is determined to have been shadowed (random number < probability shadowed), the radical is placed on the first site surrounding it and found higher than it; otherwise, it is placed in the initially selected site. This approximation does not take into account stacks two stacks away from the site and thus becomes a local effect.

b. Global

More global shadowing effects such as caused by trenches can be accounted for. The model handles shadowing of sites in a trench with the selection of the initial landing site of the radical before the local shadowing is considered. As shown in Figure II-11 each site has a certain angle at which a radical can come incident to the substrate and strike that site. This acceptance angle is calculated for each site in two dimensions given a linear trench. The argument then is that sites with a larger acceptance angle are more likely to receive an incident radical and sites relative to each other will accept more incident radicals or less incident radicals in the same proportion to their

angles of acceptance. Also the radical is approaching the surface at any angle from 0^o to 180^o with equal probability.

More formally , as shown in Figure II-12a, the acceptance angle associated with each site is calculated. From these acceptance angles a probability density is generated vs. site location. That is, the sum of all of the site acceptance angles is divided into each site acceptance angle to obtain the probability a radical will land at that site. From the probability density, a probability distribution function (Figure II-12b) is formed which is used with a random number generator to pick a site with probabilities determined by the physical features of the trench.

A number is chosen between zero and one and the site whose cumulative probability is closest to and less than the random number is the one chosen for a radical to land. In interpreting the distribution function, one looks for lines with a large slope and concludes that sites under the larger slopes are more probable sites for a radical to land because they span more of the possible range of random numbers. Looking at the distribution function, one sees very steep lines at the two ends which correspond to the top of the trench. Global shadowing is independent of and occurs before the local shadowing effect which considers only nearest neighbors.

It should be mentioned that the probability distribution is not recalculated after the start of the simulation. Even though the film is growing and the geometry of the trench may be changing, the model assumes that the shadowing algorithm should not be updated.

3. Allowed movement

The algorithm for determining the geometric shadowing of a given site uses the eight surrounding sites. This choice is made since the radical, once it adsorbs onto the surface, is assumed to be able to move and to possibly bond to any of the eight surrounding sites adjacent to it (bonding also occurs directly above and below a site). Radical movement is random. A random number is selected and is matched to one of eight equal intervals between zero and one which coorespond to eight equally probable directions. Whichever interval the selected random number is in is the direction the radical will take for that Δt_{mov} interval. For the next Δt_{mov} time interval another direction for the radical is selected, etc.

To deal with radicals moving off the substrate when a trench is **not** considered (i.e., global shadowing is turned off) a periodic boundary condition is imposed on the substrate. A radical moving off one side of the wafer is put on the other side of the wafer as shown in Figure II-13.

When deposition on a trench is considered the boundary conditions along the trench axis are changed from periodic to reflective boundary conditions while on the off axis the periodic boundary conditions are retained. Imposing periodic boundary conditions on a trench would necessitate the simulation of the complete trench to retain continuity of the boundary conditions, since simulating growth on half of the trench feature causes a discontinuity at the bottom of the trench.

4. Barriers

Once a radical has been adsorbed onto the surface, the radical moves subject to the hierarchy of timed mechanisms. As it moves in one of eight possible directions, it tries to find a site under it which has a free OH radical with which to undergo the interlinking reaction. If in its random movement on the simulation surface it finds an OH to react with and the reaction probability allows it, a bonding reaction occurs.

As the radical moves consideration is given to the barriers it may encounter. Figure II-13 shows the various situations which may arise. If the barrier is not too high, the radical attempts to bond to its side. If the radical fails to bond (determined by the reaction probability and available OH group), a check is made to determine if the radical is in a hole. A hole is defined as a surface site which has the eight stacks surrounding it all higher than it. If the radical is in a hole, an attempt is made to bond with the site underneath it with a reaction probability of unity. This in conjunction with the fact that all surface sites have retained an OH group pointing up (except BXXX) insures integration of the radical into the film. Otherwise, if the radical is not in a hole, and does not have the probability to bond to the side or the site the radical is trying to bond to does not have any free OH groups, it goes off in another random direction.

A barrier that is too high occurs where the radical "sees" a site which has already been buried. The only option is to randomly move the radical to its next site since it can not bond to a site it has no information on. Before it is moved on, the site is tested to see if it is a hole. If it is,

again the radical attempts a bond downward with reaction probability one. If it is not, the radical moves on to an adjacent site. Tests were performed to insure that results of the simulation did not change with stack height to insure these effects are not prejudicial.

In these rules for barrier engagement, a conscious attempt is made to assure a somewhat smooth film is always growing. Bonding to the side of barriers and filling up a hole whenever possible reflect the desire to make the film smooth. Having an OH group reserved for a vertical bond insures that the film will always grow.

These are only aids, however, and not sufficient to insure smooth continuous film growth. That is, a radical with no surface mobility ($P_r = 1$) can not improve the smoothness of the film by being allowed to bond to a side or in a hole since a radical with $P_r = 1$ bonds only to the site it lands on. With $P_r = 1$ or zero mobility, the surface roughness will be dictated by the "roughness" of the sites on which the radicals initially strike. In general then, conformality or smoothness of the film is highly dependent on the mobility of an adsorbed radical and residence time. Other issues such as side bonding and hole filling become important only if the radical has some initial mobility.

There is no insurance that the wafer will continue to grow if an OH group is retained at every site given the existence of BXXX on the surface. BXXX has no OH group to retain and cannot be bonded to. When the plasma has high $SiX_3(OH)$ radical content, film growth becomes dependent on the X group removal processes which create the OH groups needed for the upward bond.

III. DISCUSSION

The base case for the simulations carried out has the following parameters: a radical mix of $Si(OH)_4$ / $SiX(OH)_3$ = 0.9/0.1, $\Phi_{rad}=10^{16}$ $cm^{-2}s^{-1}$, $\Delta t_{res}= 10^{-6}$ s, $\Delta t_{mov}= 10^{-3}$ s, and $P_r=3x10^{-4}$. Properties of the simulated film to be discussed include growth rate, OH and X fractions, conformality, and roughness.

A. Growth Rate

The growth rate has a maximum value determined mainly by Φ_{rad}. In general, mechanisms which cause fewer incident radicals to integrate into the film per unit time cause a decrease in the maximum growth rate. A good indication of this effect is the integration probability P_i, which is an indication of the likelihood an adsorbed radical bonds before desorbing. A higher probability is equated to larger growth rates since a high number of radicals will bond to the surface. As P_i decreases, the radical flux has to supply more radicals to eventually obtain the same number of radicals incorporated into the film since a higher number are desorbing.

In general, increasing the growth rate can be achieved by increasing the residence time, by raising the reaction probability P_r and, of course, increasing Φ_{rad}. Also, when applying the temperature scalings of the timed processes, the growth rate increases with decreasing temperature.

1. Residence time

The growth rate vs. Δt_{res} is shown in Figure III-1 and shows that a shorter residence time lowers the growth rate. That is, decreasing the residence time decreases the number of attempts a radical can make when trying to integrate into the film before being desorbed from the surface. This leads to a higher number of radicals incident on the substrate which are unable to incorporate into the film and as a result eventually desorb from the film. The result is the need for more radicals to come down to the surface to grow the layers of film, which takes more time and thus lowers the growth rate. Figure III-1 has a plateau for large Δt_{res} values, which is the regime in which the integration probability P_i approaches unity since there are a large number of possible moves the radical can make on the surface.

2. Reaction probability

Another parameter which may increase the number of radicals being desorbed from the surface and thus lower the growth rate is P_r. A plot of growth rate vs. reaction probability is shown in Figure III-2. As P_r is initially lowered, it is not yet low enough to affect P_i. With P_i very near unity, every radical incident on the substrate becomes integrated into the film. At a certain threshold, however, lower values of P_r lower P_i from a near unity value so some of the radicals on the substrate surface desorb. Also shown is the effect of increasing the residence time which lessens the effect of P_r in the range considered since each radical has more opportunity to bond.

3. Radical flux

A plot of growth rate vs. Φ_{rad} is shown in Figure III-3, and displays an increasing growth rate with increasing Φ_{rad}. The results show that increasing the source of radicals to the surface increases the growth rate. Since the standard parameters were used, the rates shown are not the maximum possible for the given Φ_{rad}. The plot also shows a larger residence time corresponds to faster growth rates. Since radicals on the surface do not "see" each other, the resulting plot is linear. If some of these effects were included, the results would be less linear with the growth rate not increasing as rapidly with the flux.

4. Temperature

The simulated growth rate vs. temperature plot (Figure III-4) has a negative activation energy of -0.11 eV which is higher than the values observed by C. S. Pai and C. P. Chang[12] (-0.12 eV) and by B. L. Chin and E. P. van de Ven[1] (-0.19 eV). The negative activation energy is believed to be due mainly to the smaller residence time at higher temperature and in the model is the only process considered which lowers the growth rate for larger T.

Most opinions on the cause of the negative activation energy center on plasma effects. A model developed by G. B. Raupp and T. S. Cale[24] asserts that the recombination of O radicals at the wall to form O_2 increases with temperature resulting in fewer O radicals to react with TEOS to form the film. Their model concentrates on the evolution of oxygen in its various states in the plasma, and uses a computed sheath potential to get the flux of oxygen ions that are reaching the surface. The oxygen flux arriving on the surface reacts with TEOS to form the oxide. The

reduction of O radicals with increased temperature reduces the oxygen flux to the surface and lowers the growth rate.

B. Fraction of X Groups

The fraction of X groups (C_2H_5O) in the film is a function of three parameters. The first is the type of radical incident on the substrate with $SiX_3(OH)$ contributing more to the fraction of X in the film if integrated than $SiX_2(OH)_2$, $SiX_2(OH)_2$ contributing more than $SiX(OH)_3$, etc. The second is the oxygen flux which supplies oxygen to the surface reducing the number of X groups and increasing the number of OH groups. The third is pyrolysis in which X groups become OH groups and release C_2H_4.

1. Oxygen flux

Figure III-5 shows how the X fraction varies with Φ_{oxy}. For low values of Φ_{oxy} the X fraction is the same as that in the radical flyux. As Φ_{oxy} is increased to around the same order of magnitude as Φ_{rad} (10^{16} $cm^{-2}s^{-1}$), the process begins to have an effect on the X fraction. At around $5x10^{16}$ $cm^{-2}s$ or less than a magnitude above the Φ_{rad} value, the process has essentially eliminated the presence of the X group. Little variation is seen between the near and buried layers.

2. Pyrolysis

Figure III-6 shows the X fraction vs. Δt_{pyr}. Again there is a threshold effect, but in this case the process begins to have an effect on the X fraction at rates two magnitudes slower than the incoming radical process rate, as opposed to Φ_{oxy} which has to be within a magnitude of Φ_{rad}. Another difference is the separation of the near and buried levels by as much as 2-3%. The near level has more carbon content than the buried level given the smaller time a radical has spent as a part of the silicon network. The shorter time gives the radical less of a chance to lose X groups through pyrolysis. The buried X eventually levels off to zero when the pyrolysis rate is equal to the incoming radical rate ($\Delta t_{ads}=10^{-4}$ s) with the near X group fraction still sloping towards zero.

C. Fraction of OH Groups

Incident radical types, interlink, and void formation play a role in the presence of OH groups in the film. Figure III-7 shows how the fraction of OH is affected by the interlinking process. The OH fraction is found to have a large error scatter when changing a random number

seed. The general trend however seems valid. At the high end of the curve, the interlink process is essentially off and the OH fraction reflects silicon sites keeping either two of their four OH groups ($Si(OH)_4$ radicals) or one of their three ($SiX(OH)_3$ radicals) with there being no way to eliminate them. As the interlinking process is started and made faster, the OH fraction drops. At high rates of interlinking, the lower plateau is reached which is a consequence of retaining an OH group on all of the surface sites. The buried OH fraction is almost zero since sites are allowed to interlink if possible before being buried.

D. Conformality

Conformality is a measure of how well a film mimics the variations in height of the substrate it is grown on. If trenches are considered, good conformality is usually equated to having the ratio of side thickness and bottom thickness to top thickness near unity. Depending on the use however, having B/T (bottom to top) ratios near unity and some growth on the side is accepted. If the concern is to completely fill a trench to create a planar surface, one looks for films which grow with positive (as opposed to negative) slopes so that a large hole or void will not form that might be uncovered in future etching steps. A film with a positive slope has the film thickness on the sides of the trenches thicker on the bottom than on the top.

Conformality in the simulations become worse as radicals visit fewer sites. Radicals visiting a large number of sites move around a larger part of the surface and thus are able to integrate into sites receiving lower fluxes whereas radicals visiting fewer sites are not able to spread out from each other to any great extent. In terms of the model, radicals need a long residence time and a low reaction probability to allow greater movement and thus better conformality.

Another factor affecting the conformality of a film is the physical features of the trench. The physical features can cause the radicals to fall mainly on the top of the trench and thus the conformality becomes even more highly dependent on the radicals' movement radius.

All of the following conformality data use the global shadowing probability distribution, reflective boundary conditions along the trench axis, and periodic conditions on the off axis with the deposition stopping when the average height across the whole trench is 15 layers.

1. Aspect ratio

The aspect ratio convention cited here is the ratio of the height of the trench to the width. A trench with a high aspect ratio will shield the bottom of the trench (based on acceptance angle) to a greater extent than a trench of lower aspect ratio; thus, the bottom of the high aspect ratio trench relies on radicals already adsorbed on the surface to find their way to the bottom instead of radicals incident from the plasma.

As Figures III-8 and III-9 show, the more extreme topographies give less conformality as measured by side and bottom to top height ratios (values are all averaged heights of the specific regions). Improvement of the conformality is achieved by smaller reaction probabilities as shown in Figure III-8 and by larger residence times as shown in Figure III-9.

Experimentally measured conformality is found to worsen with increased aspect ratios with B/T > S/T (B/T≈0.9 to 0.6 and S/T≈ 0.6 to 0.2).[13] Although for more directional depositions where B/T is near unity and S/T is very small the ratios are less sensitive to the aspect ratio.[25] There are also cases (low frequency plasma[26] and downstream plasma reactor[12]) in which the sidewall thickness is greater than the bottom thickness.

2. Reaction probability

A more direct display of the effect the reaction probability P_r has on the height ratios is shown in Figure III-10 for an aspect ratio of 1.42 and in Figure III-11 for an aspect ratio of 0.25. In both cases the conformality approaches unity as P_r is lowered. However, it is also shown that there is a limit (dependent on the residence time) to how much P_r can be reduced to improve the ratios. The shorter the residence time the higher the reaction probability at which conformality saturates. The ratio saturates when the reaction probability is low enough so that the mobility of the adsorbed radicals is limited by the maximum number of sites visited or the residence time allowed on the surface. Essentially all of the radicals are achieving the maximum distance they can travel from their landing point; that is, the ratios approach a value representing the best conformality that can be achieved for that aspect ratio given the reaction probability and the residence time.

Figure III-12 shows plots of stack heights vs. site position for half of a trench of aspect ratio 0.25 and how the heights vary with P_r. The x-axis and y-axis are not to scale. The three

regions on the stack height vs. position plot labeled A , B, and C correspond to the labeled regions of the trench. Remember that these regions are distinguished from each other in the model only by the probability that the radical lands in each particular region. Figure III-13 shows the same for a trench of aspect ratio 1.43. For the highest P_r values, the heights reflect the probability distribution used for the global shadowing with the sudden transition from top of the trench to the side of the trench in evidence. As P_r is lowered this transition becomes more gradual and, in general, complete conformality is approached.

E. Roughness

As P_r is varied from 0.3 to 0.001 Figure III-14 shows pictorially how the roughness varies on a 80x80 site slab. The slab was smooth before deposition and grown to an average height of 100 layers. Comparing these to Figures III-12 and III-13, the P_r value has to be smaller to smooth the film if there is a trench than if starting a deposition on a smooth surface.

IV. CONCLUSIONS

In reviewing the results of this work it becomes apparent that the model may not have the geometric rigor to fully address the issues of conformality in large structures and is fundamentally limited by the model's approach. The model essentially stacks blocks on a planar surface given certain rules, and the trench is simulated by the probability of where a radical is first put on the surface determined by a trench's initial physical dimensions. This approach is thus a quasi three-dimensional approach, opposed to a true conformality study which would need a true third dimension. Some weaknesses of the model are that stacks in the corners of the trench "grow through each other" since in the model they grow parallel to each other instead of perpendicular to each other as in a real trench. The model is not set up to update the global shadowing probability distribution given the absence of the third dimension. This refinement could be added. Using only initial measurements of the trench when determining the global shadowing cause the simulations results to become more inaccurate as more film is grown and the trench measurements deviate from their initial dimensions. Since radicals do not reflect from the surface of the trench a radical is unable to "bounce" into an area that may be otherwise largely shadowed from the plasma.

General improvements that could be made in the model are: have a percentage of the surface passivated by OH groups instead of all, include dangling bonds, take into account other types of integration reactions such as one involving dangling bonds, and have interactions between radicals such as adsorbed radicals encountering each other and an incoming radical from the plasma hitting an adsorbed radical.

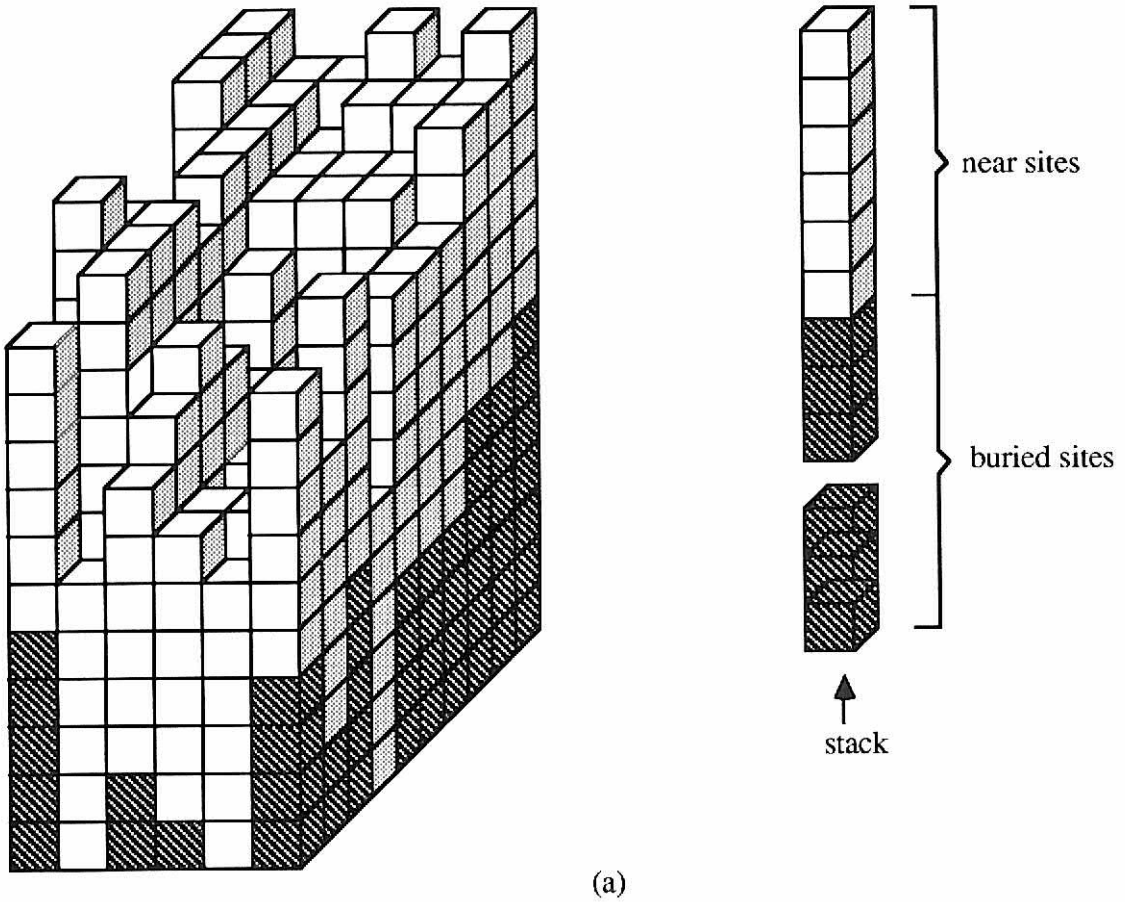

(a)

near site

buried site

- site types:
  BBBB
  BBBX
  BBBO
  BBOX
  BBXX
  BBOO
  BOOX
  BOXX
  BXXX
  BOOO
  VOID

•symbols defined:

B → — O —

O → — OH

X → — OC_2H_5

VOID → empty space

- former near site types are averaged
- not in the near site array

(b)

Figure II-1. (a) A 6x10 stack substrate with a near layer depth of 6. (b) The substrate or silicon network is made up of near sites and buried sites. The near sites are distinguishable by position and bonding history. The buried sites consist of averaged statistics of buried near layers.

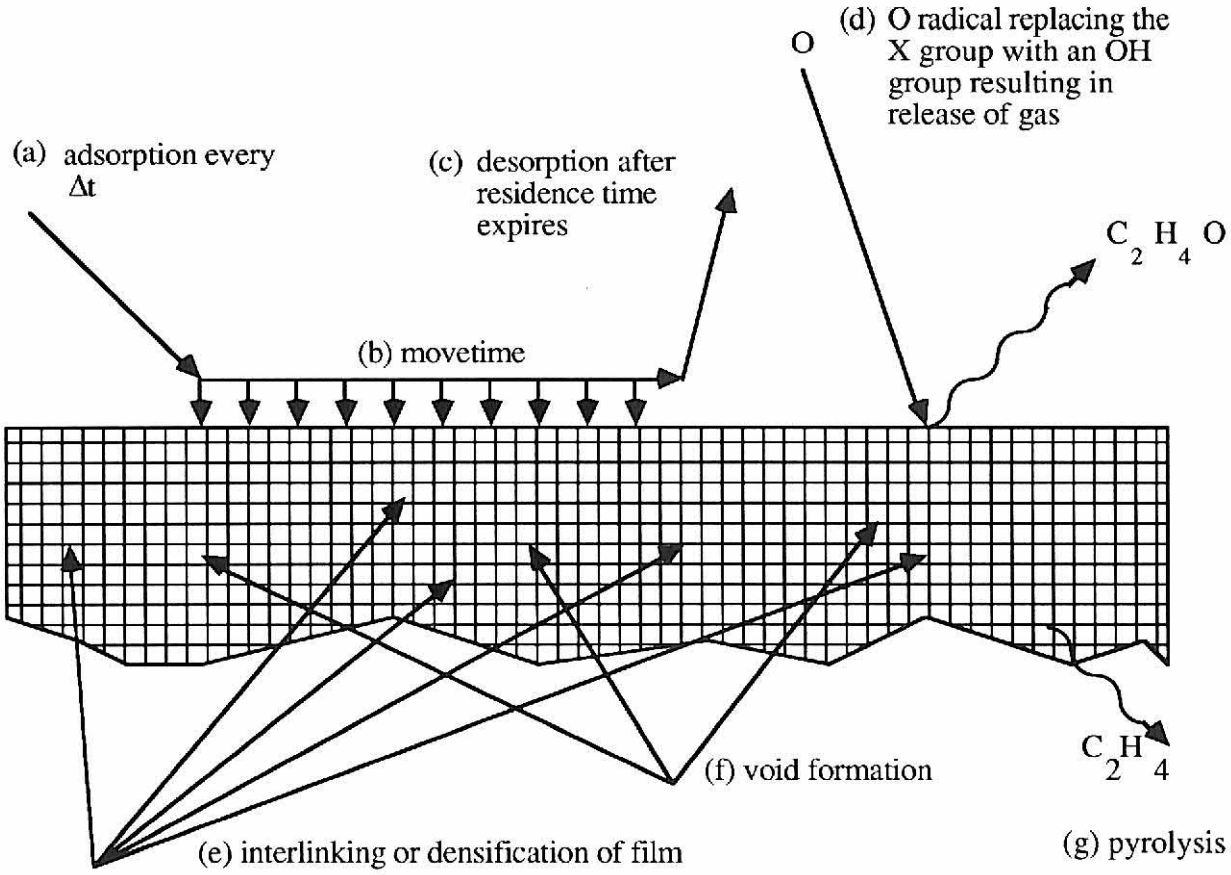

Figure II-2. The various timed processes treated in the model. Radicals coming down from the plasma (a), diffusion on the surface (b), and eventually desorbing from the surface if unable to integrate into the film (c). O radicals come down from the film (d) and react with the X groups. In the substrate there is interlinking (e) which reduces the OH content and increases the number of bonds, also there is void formation (f) which is similar to interlinking but also forms holes in the film as well. Last there is pyrolysis (g) which is a thermal process which reduces the amount of X groups in the film.

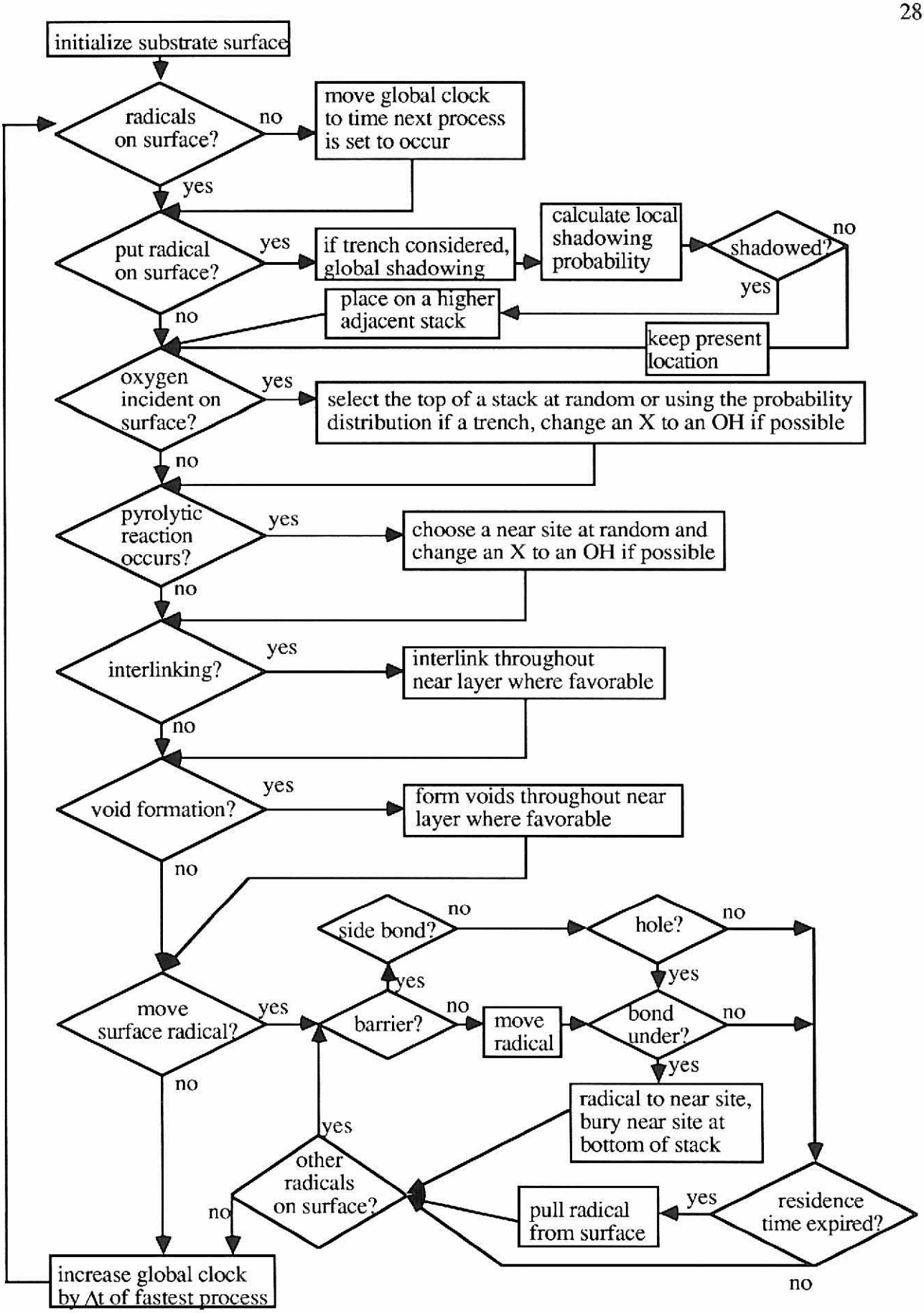

Figure II-3. Flow chart of the various processes in the model.

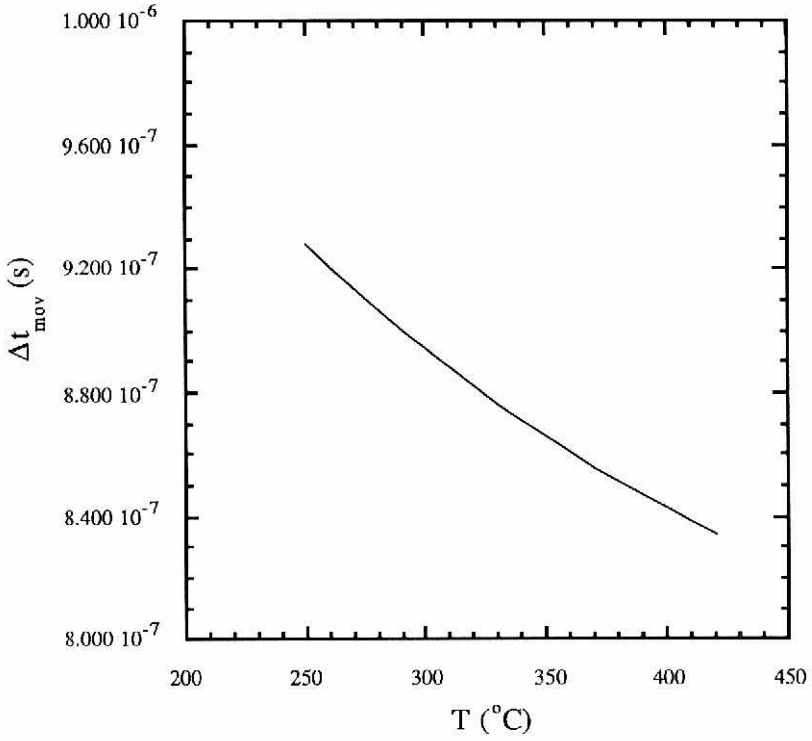

Figure II-4. Move time Δt_{mov} vs. temperature.

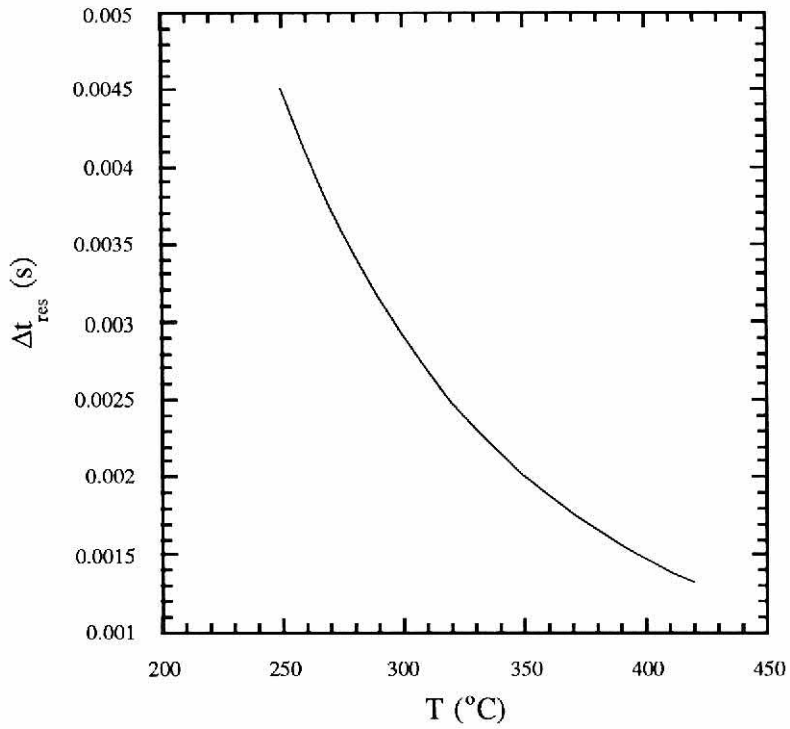

Figure II-5. Residence time Δt_{res} vs. temperature.

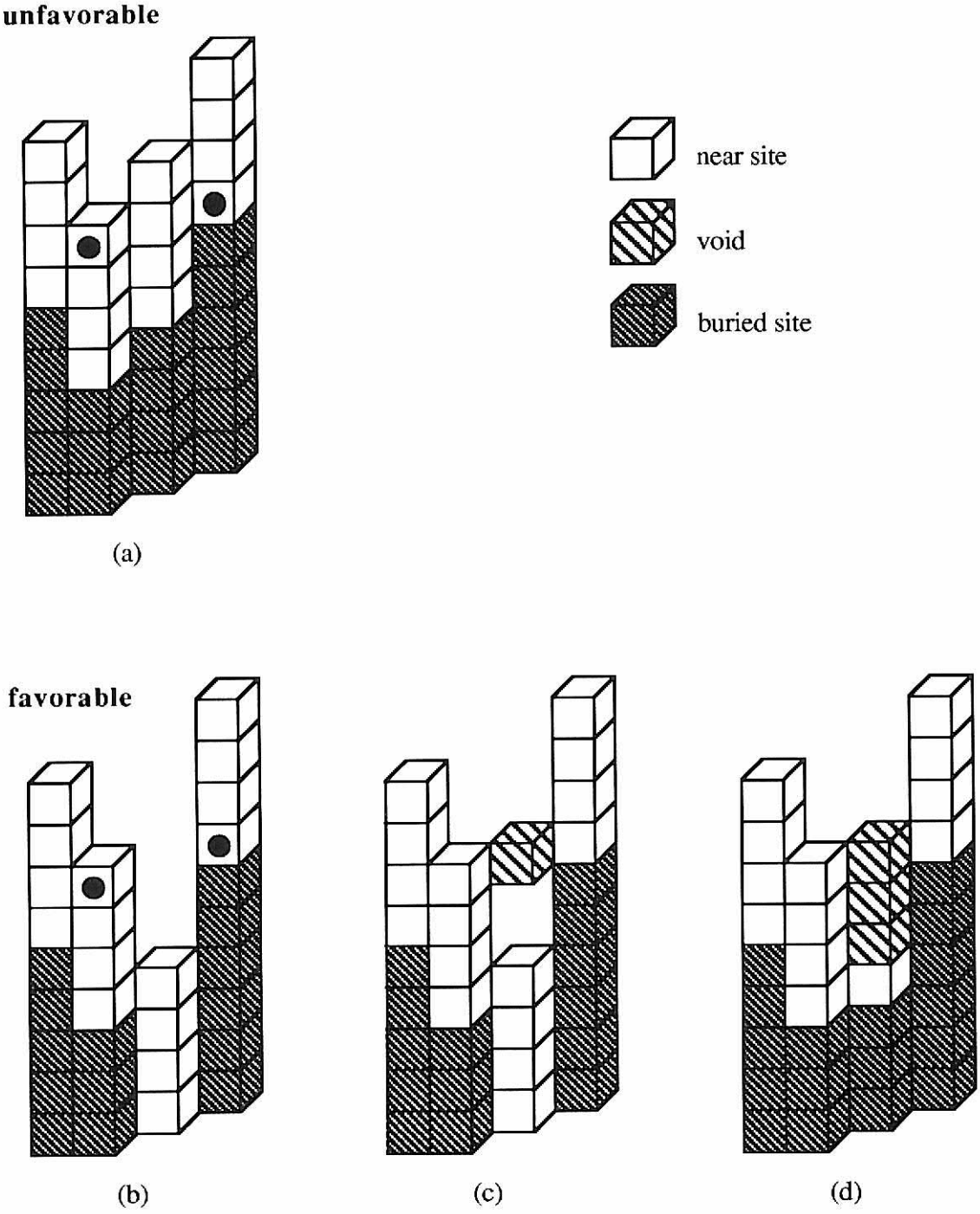

Figure II-6. An unfavorable condition (a) for void formation. Favorable conditions are (b) two sites with available OH groups a stack away and separated by empty space. When allowed, (c) a void forms between the two sites and (d) all empty sites above the stack where the initial void forms.

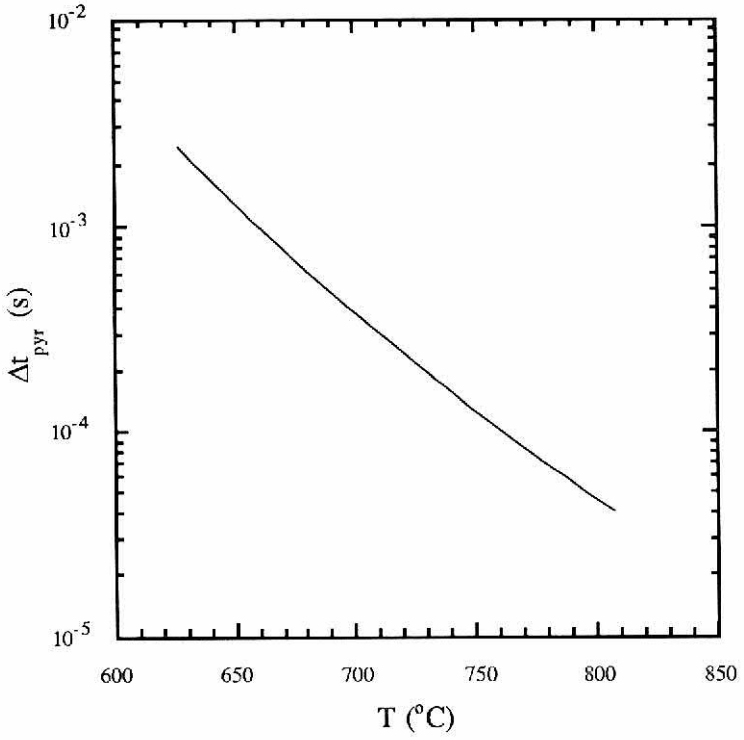

Figure II-7. Time between pyrolysis calls Δt_{pyr} vs. temperature.

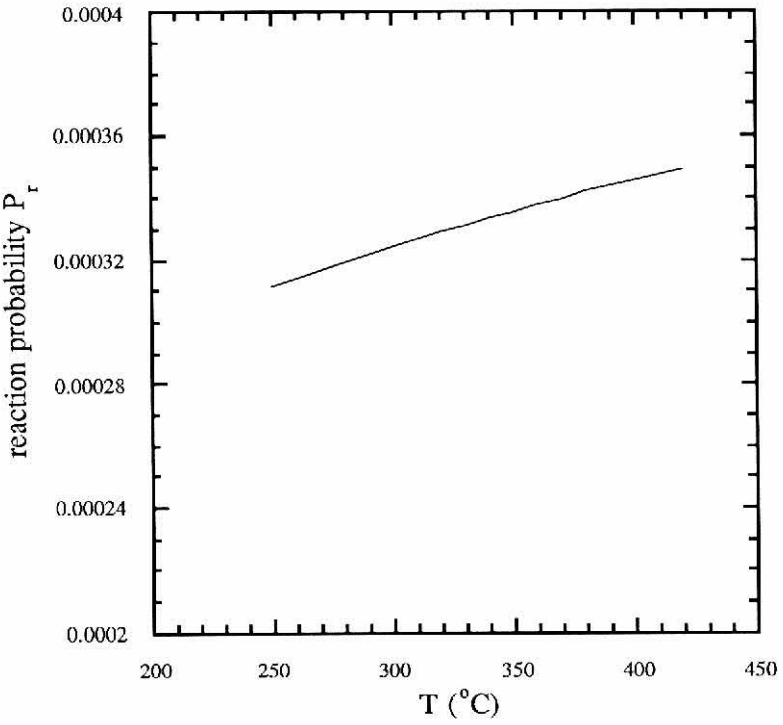

Figure II-8. Reaction probability P_r vs. temperature.

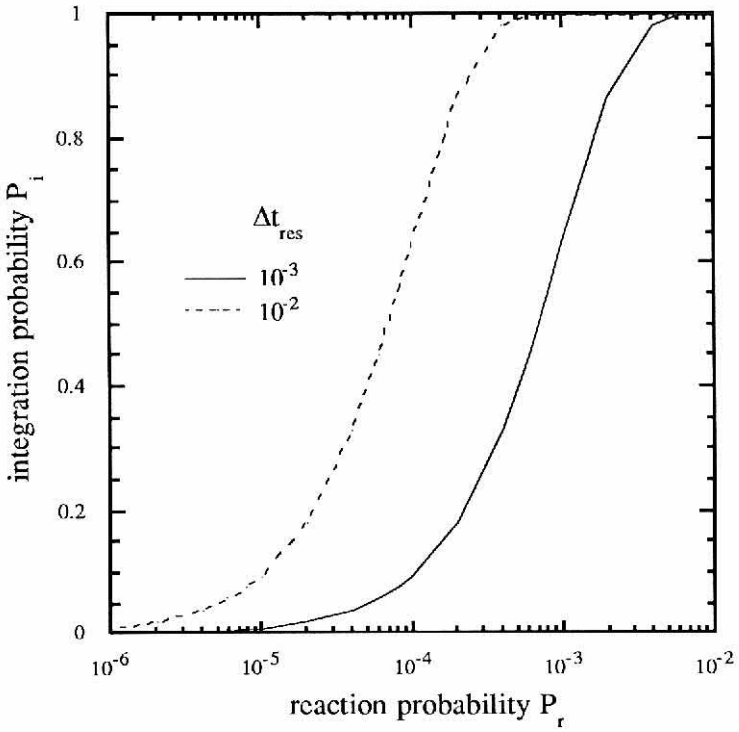

Figure II-9. Integration probability P_i vs. reaction probability P_r.

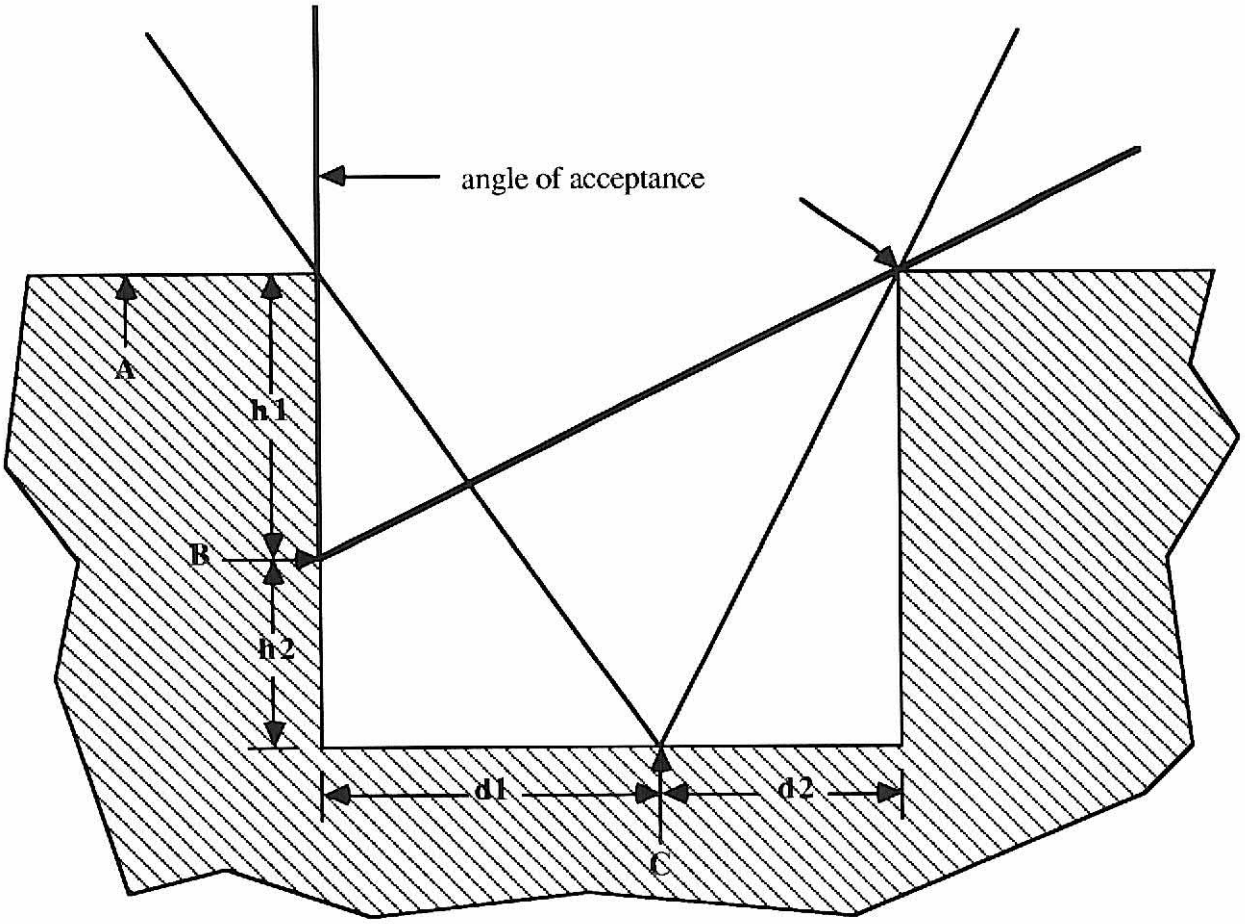

site	angle
A	π
B	arctan[(d1+d2)/h1]
C	π - arctan[(h1+h2)/d1] - arctan[(h1+h2)/d2]

Figure II-11. Global shadowing. When coverage of trench features is considered, radicals coming to the surface are more likely to land on a site with a larger acceptance angle.

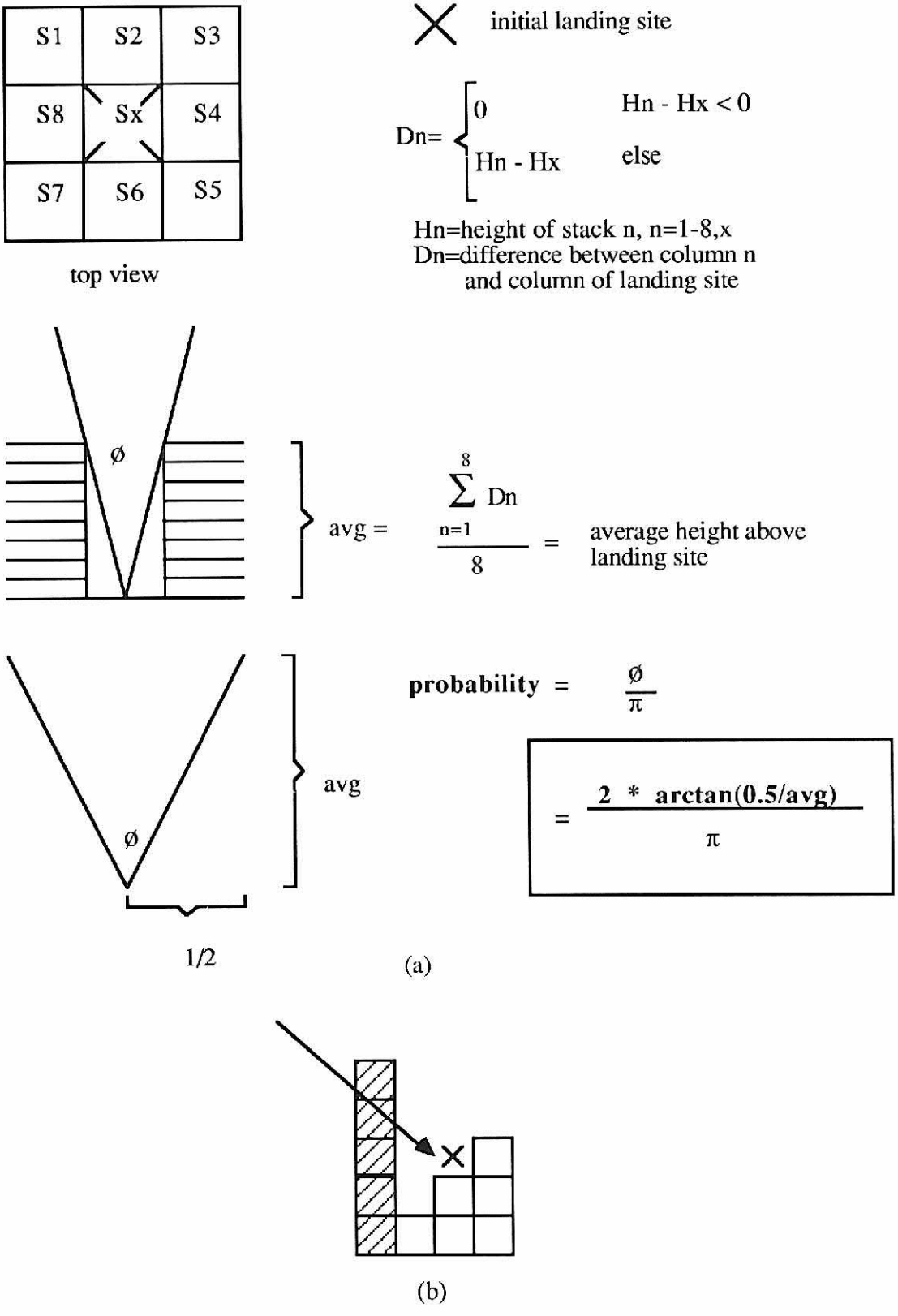

Figure II-10. (a) Calculation for the probability that an incident radical lands on a stack and is not blocked by an adjacent stack, which is used to determine if local shadowing has occurred. (b) Stacks more than one site away from the landing site play no part in the calculation even though the stacks may be shielding the landing site from the incoming radicals.

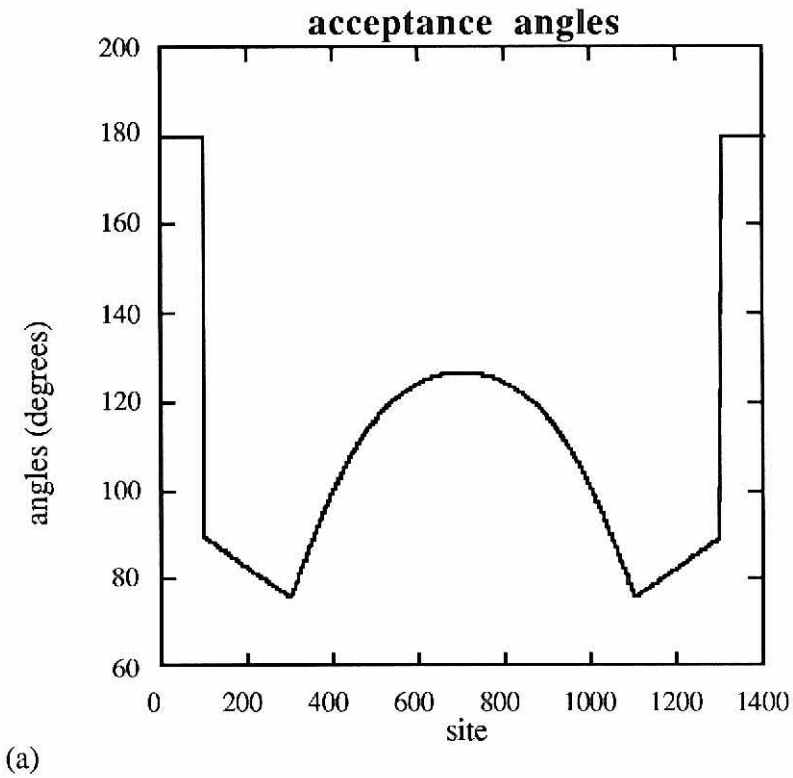

(a)

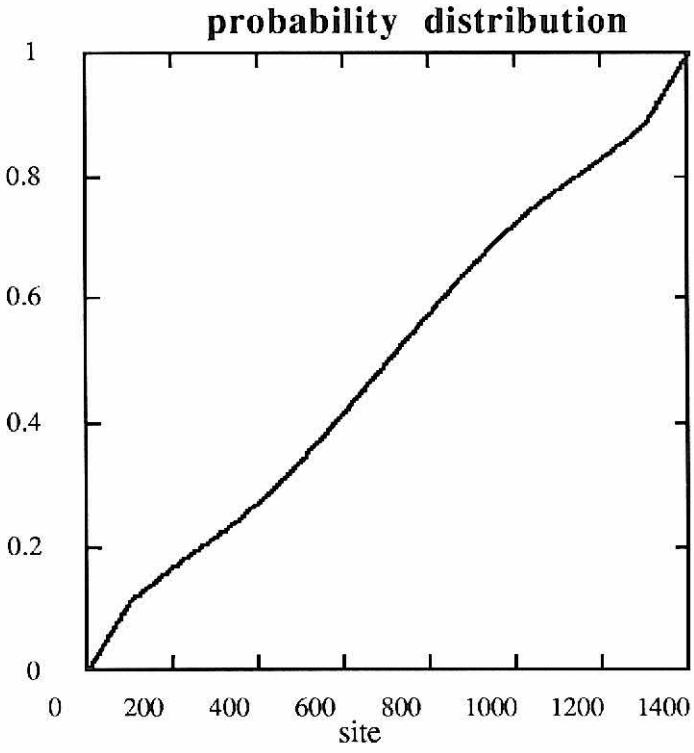

(b)

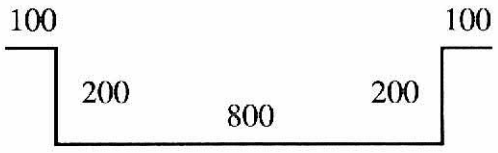

(c)

Figure II-12. Global shadowing is dealt with by using (a) the acceptance angles to generate the (b) probability distribution. (c) This is a case for a trench with aspect ratio of 1/4 with measurements given in number of sites.

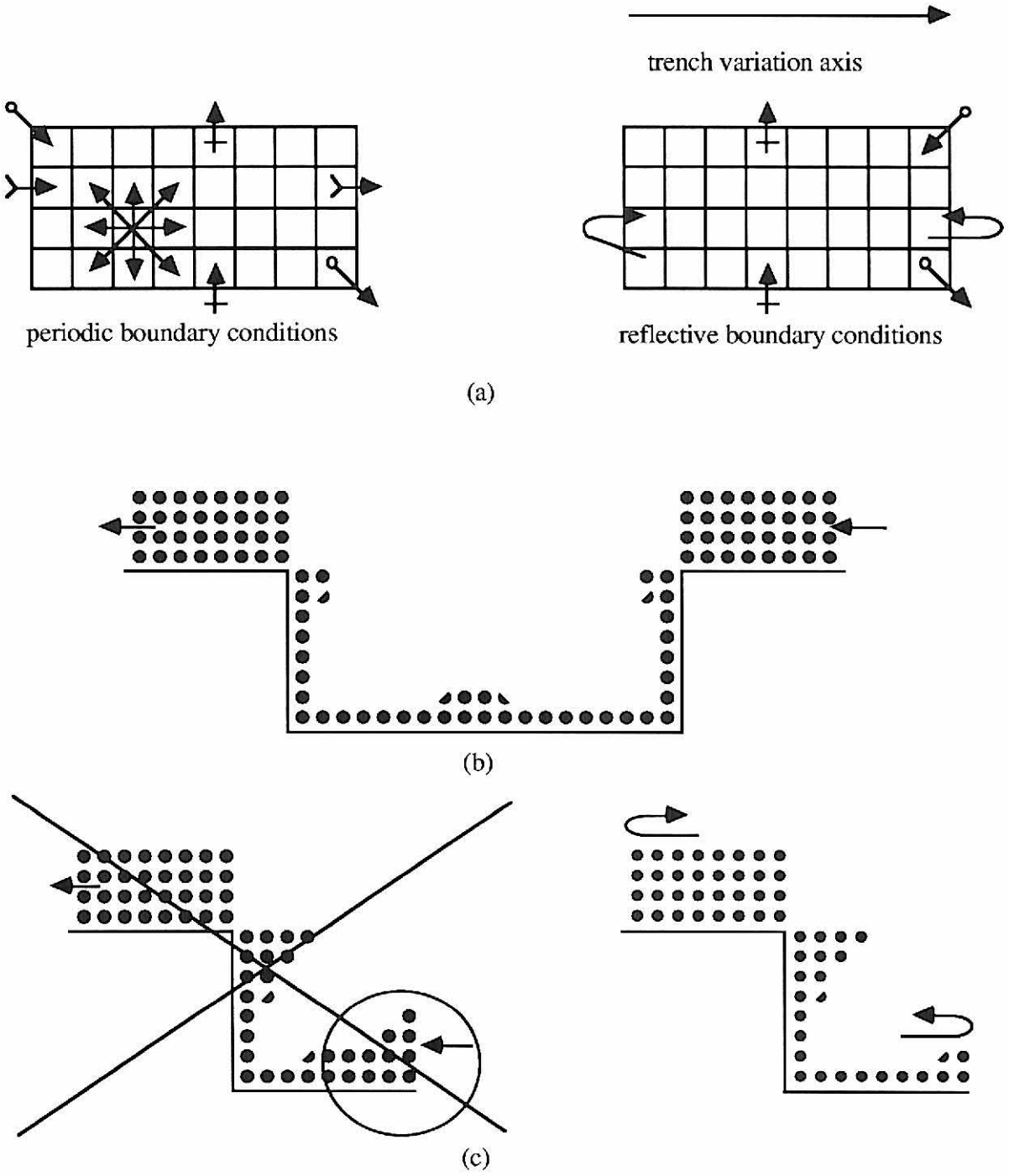

Figure II-13. A radical can move in any of the 8 directions. When moving off the substrate two different boundary conditions are used, periodic boundary conditions (pbc) and reflective boundary conditions (rbc). (b) When growth on trenches is simulated, a full trench is needed if pbc are used, otherwise (c) the boundary conditions no longer match given a site deep in the trench is next to a site on the surface. For a half trench rbc's are used to match boundary conditions.

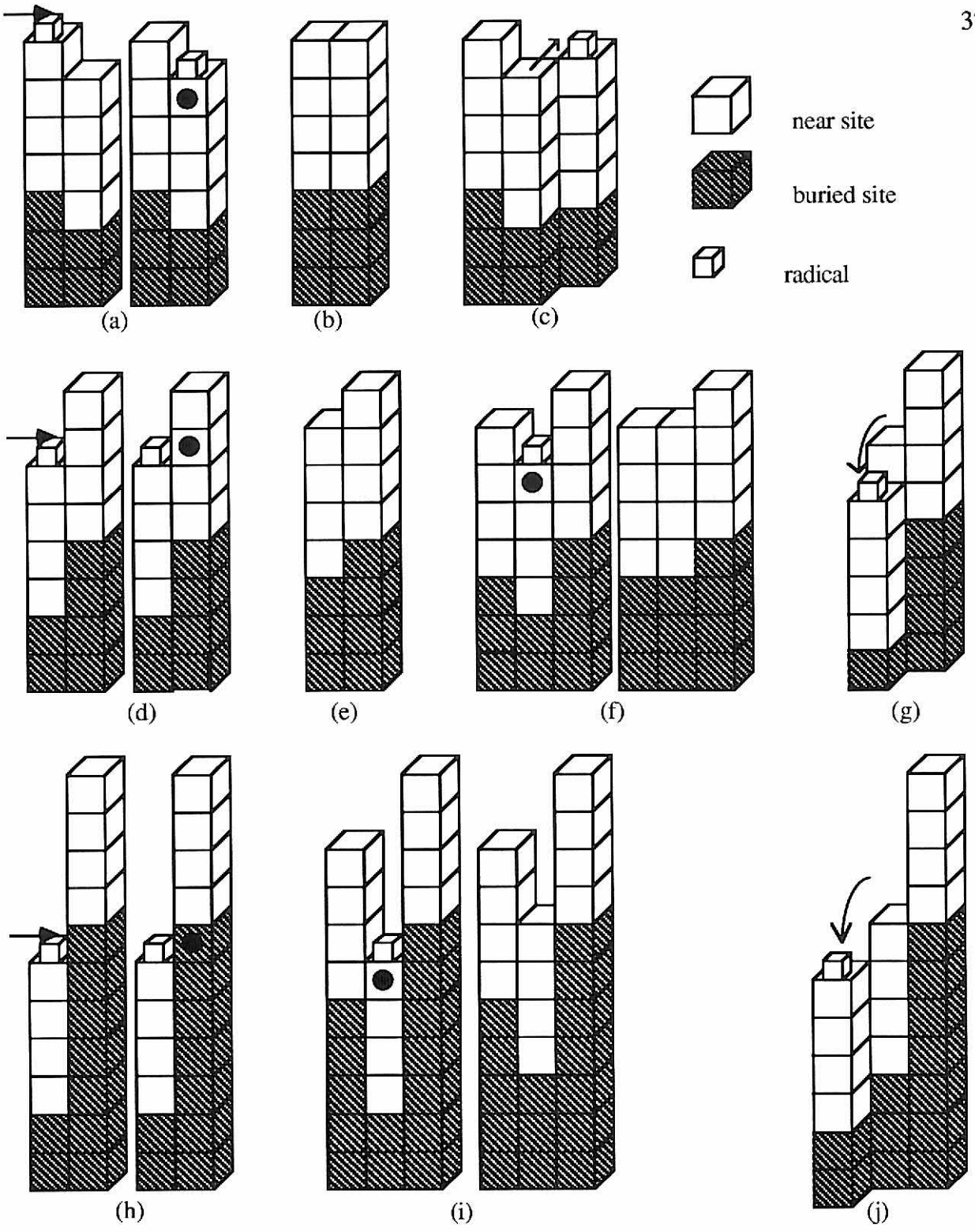

Figure II-14. Barriers. (a) No barrier? radical attempts to bond under it, (b) success, (c) failure. (d) Low barrier? radical attempts a side bond, with (e) success, (f) if in hole (8 surronding stacks higher) bonds on stack with probability one, or (g) failure. (h) High barrier? Impossible to bond to side so if not in a hole (i), moves on (j).

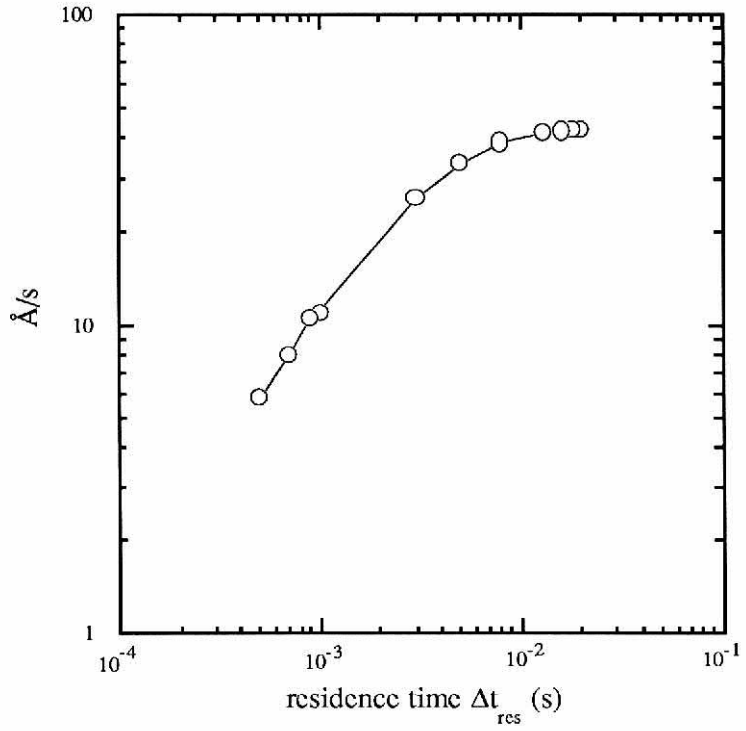

Figure III-1. Growth rate vs. residence time Δt_{res}.

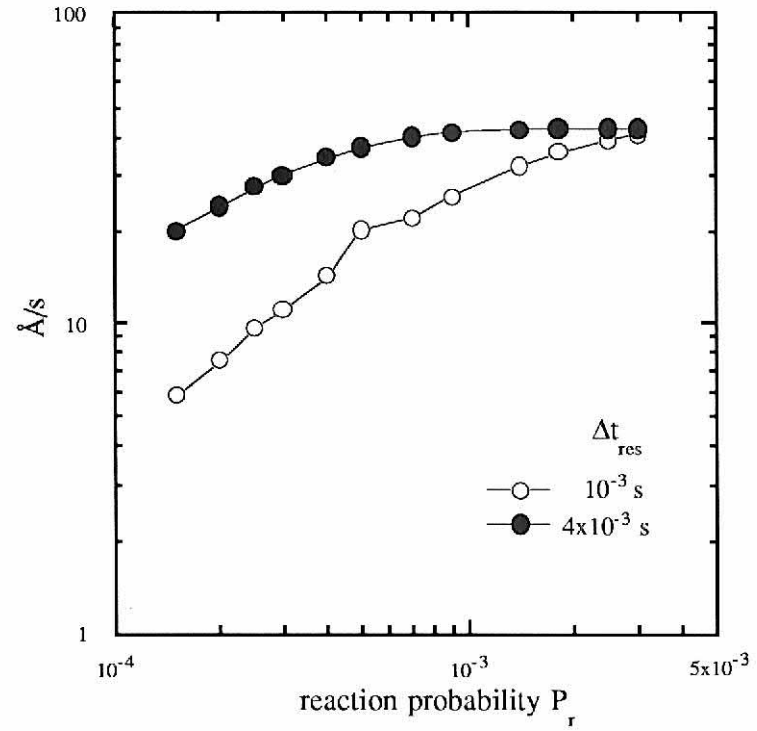

Figure III-2. Growth rate vs. reaction probability P_r for different Δt_{res}.

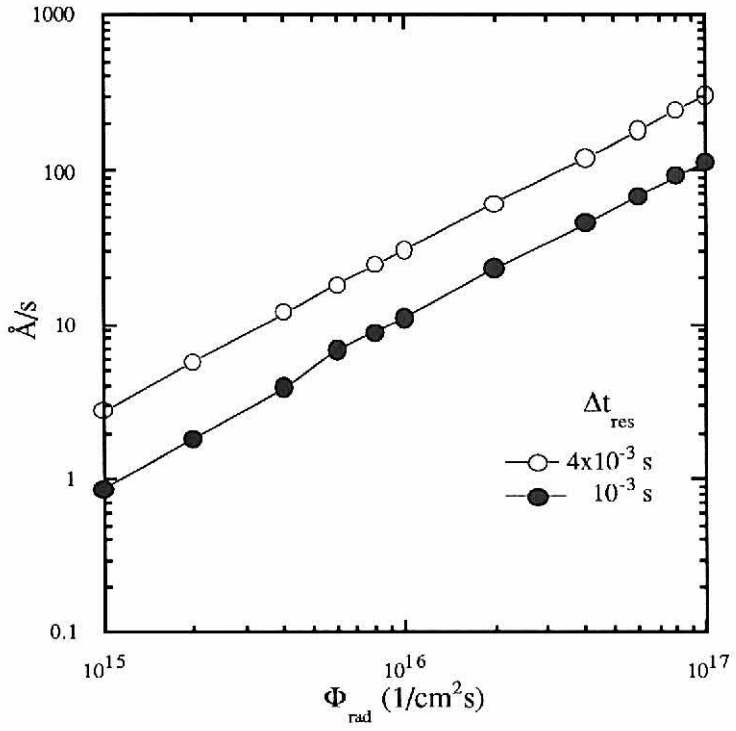

Figure III-3. Growth rate vs. incoming radical flux for different Δt_{res}.

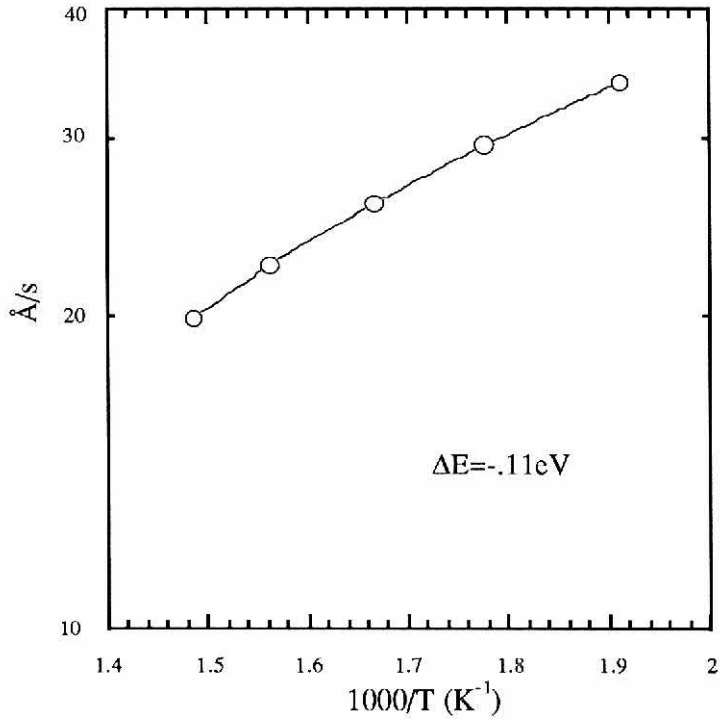

Figure III-4. Growth rate vs. temperature in K.

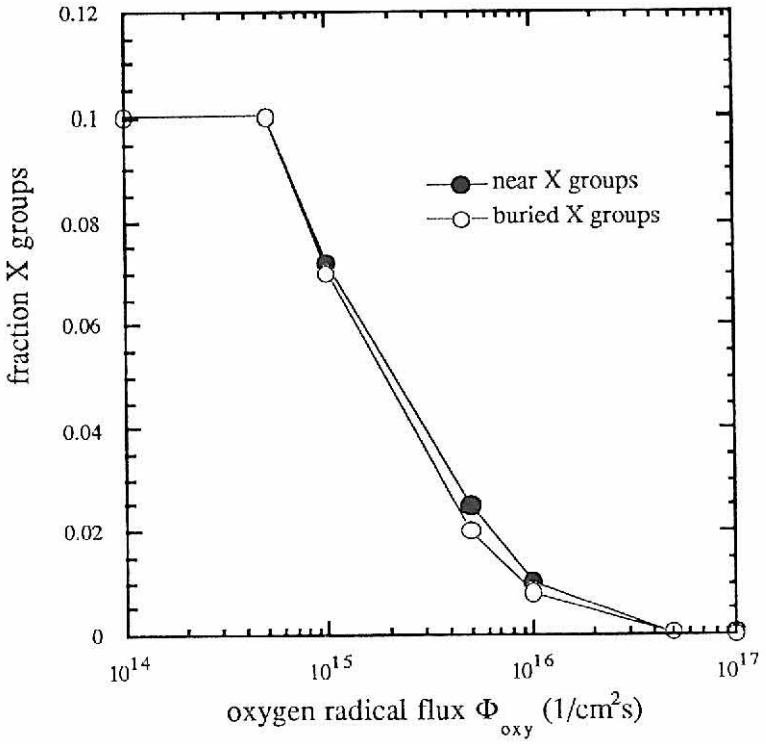

Figure III-5. Fraction C_2H_5O vs. oxygen radical flux.

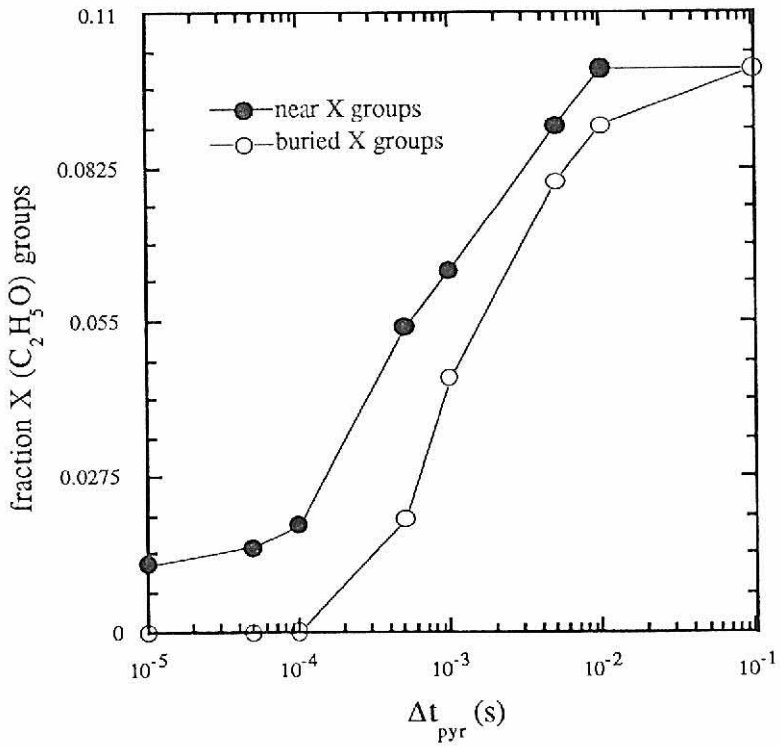

Figure III-6. Fraction C_2H_5O vs. time between pyrolysis reactions Δt_{pyr}.

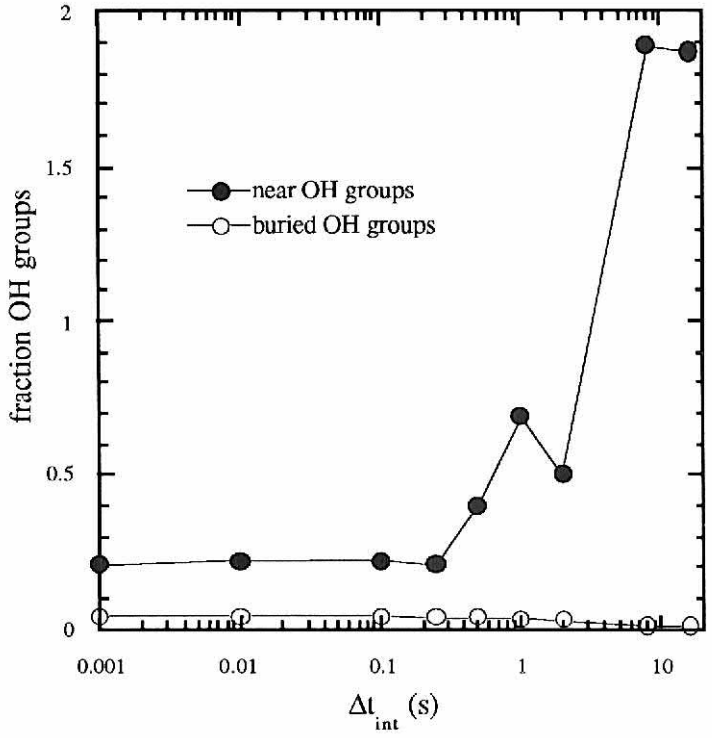

Figure III-7. Fraction OH vs. time between interlink calls Δt_{int}.

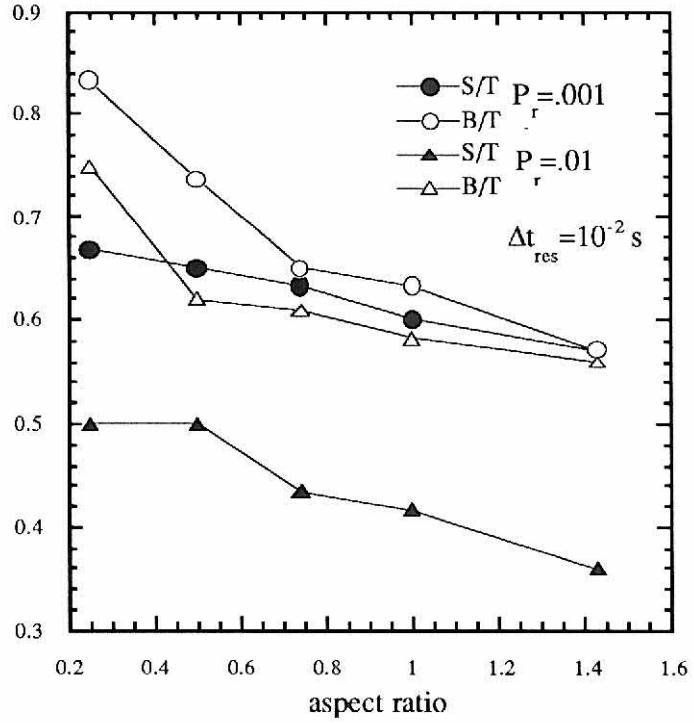

Figure III-8. Side and bottom to top average height ratios vs. aspect ratio for different reaction probabilities.

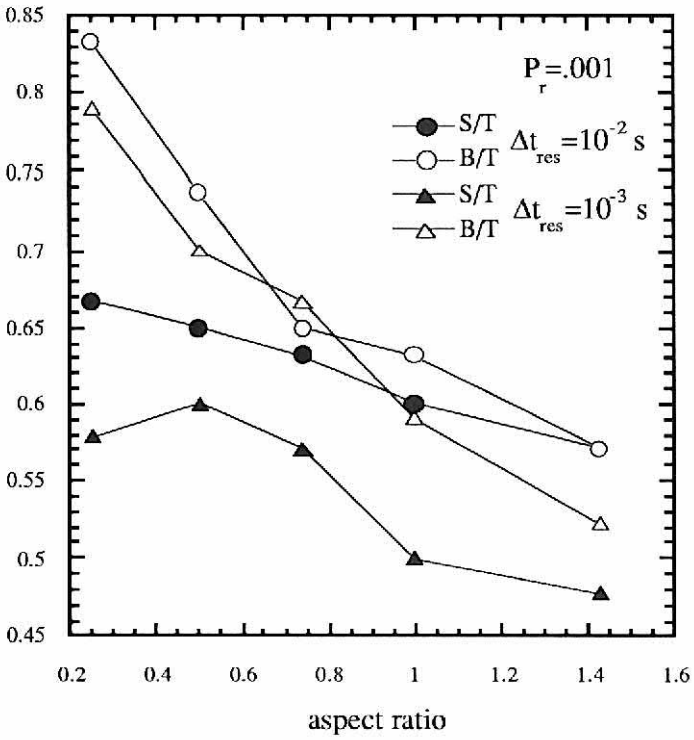

Figure III-9. Side and bottom to top average height ratios vs. aspect ratio for different residence times.

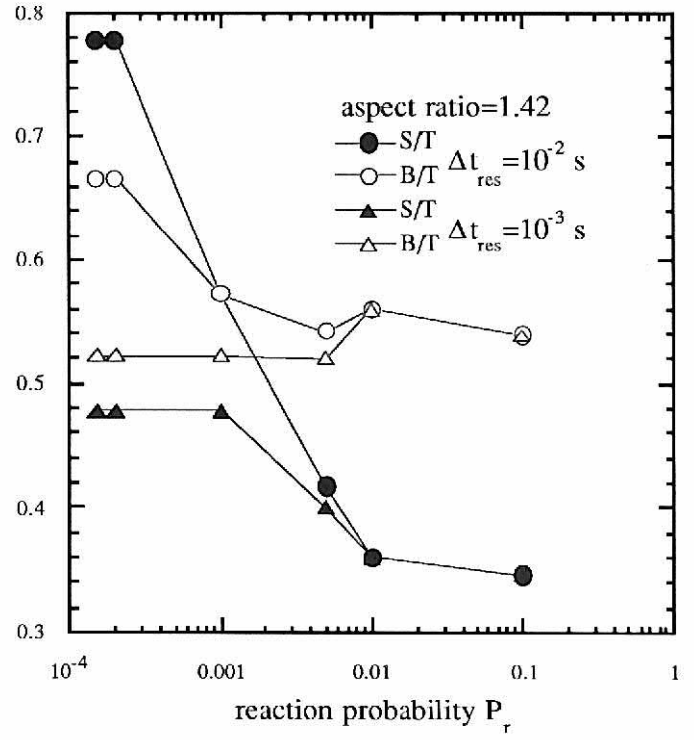

Figure III-10. Side and bottom to top average height ratios vs. reaction probability with an aspect ratio of 1.42.

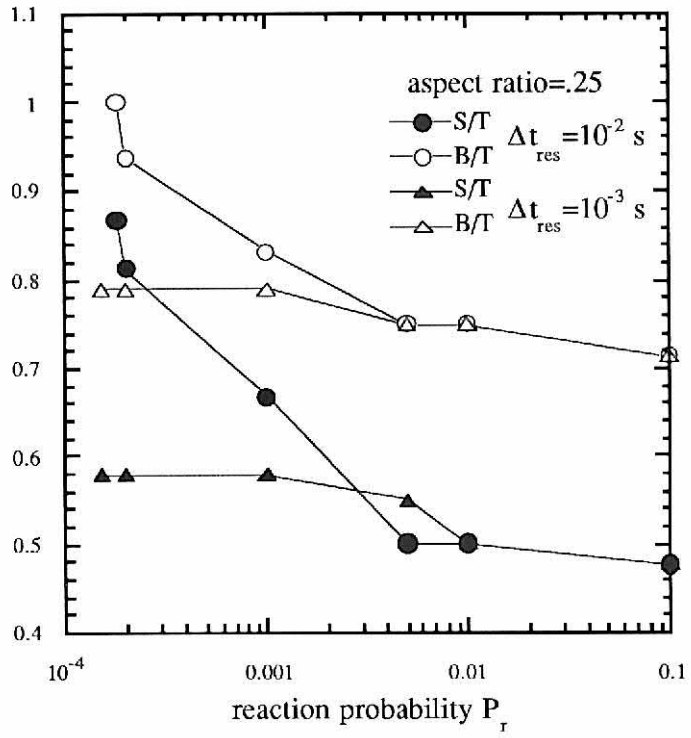

Figure III-11. Side and bottom to top average height ratios vs. reaction probability with an aspect ratio of .25.

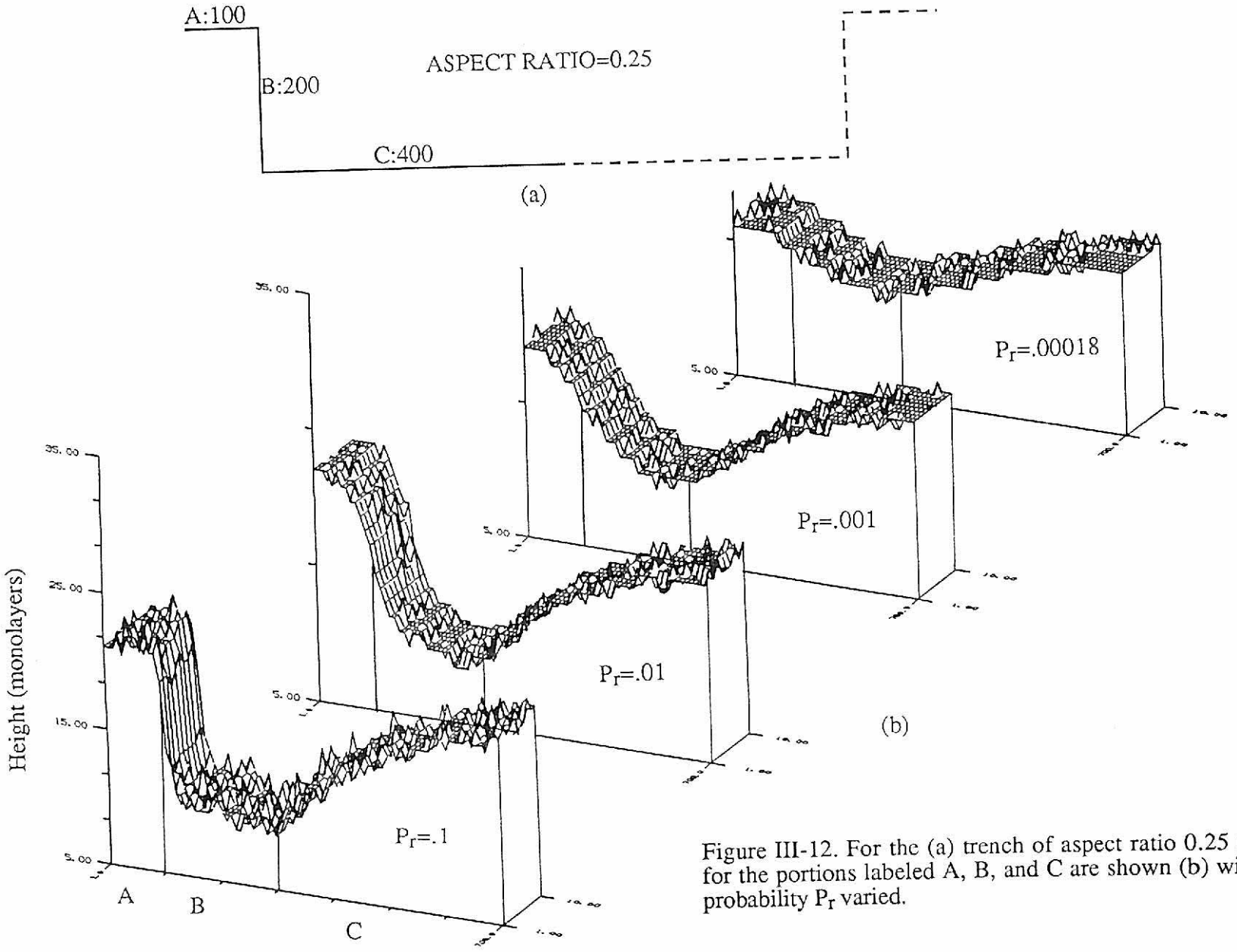

Figure III-12. For the (a) trench of aspect ratio 0.25 the heights for the portions labeled A, B, and C are shown (b) with reaction probability P_r varied.

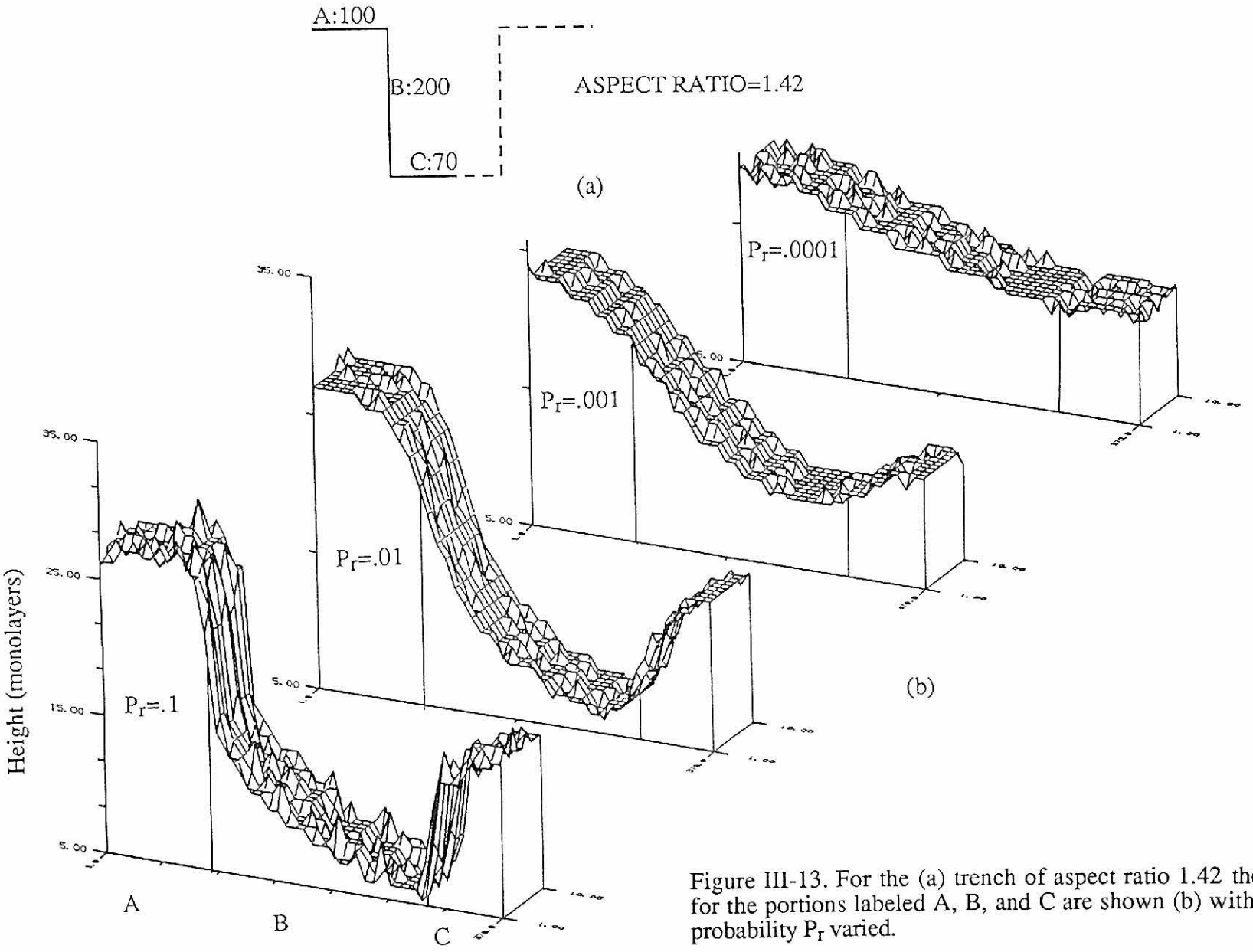

Figure III-13. For the (a) trench of aspect ratio 1.42 the heights for the portions labeled A, B, and C are shown (b) with reaction probability P_r varied.

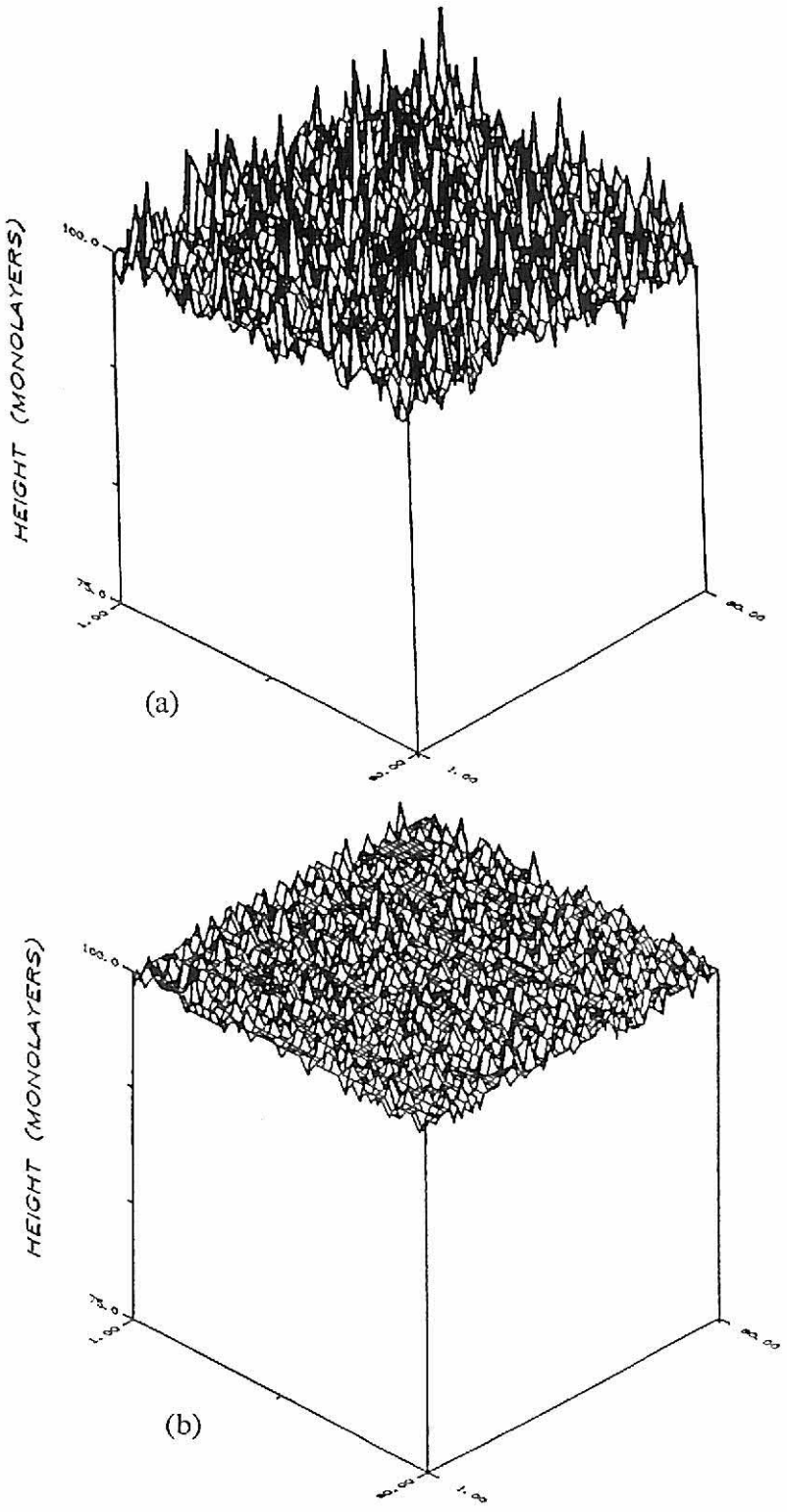

Figure III-14. Stack heights vs wafer position for growth on an initially smooth surface with P_r varied for (a) $P_r=3x10^{-1}$and (b) $P_r=10^{-1}$.

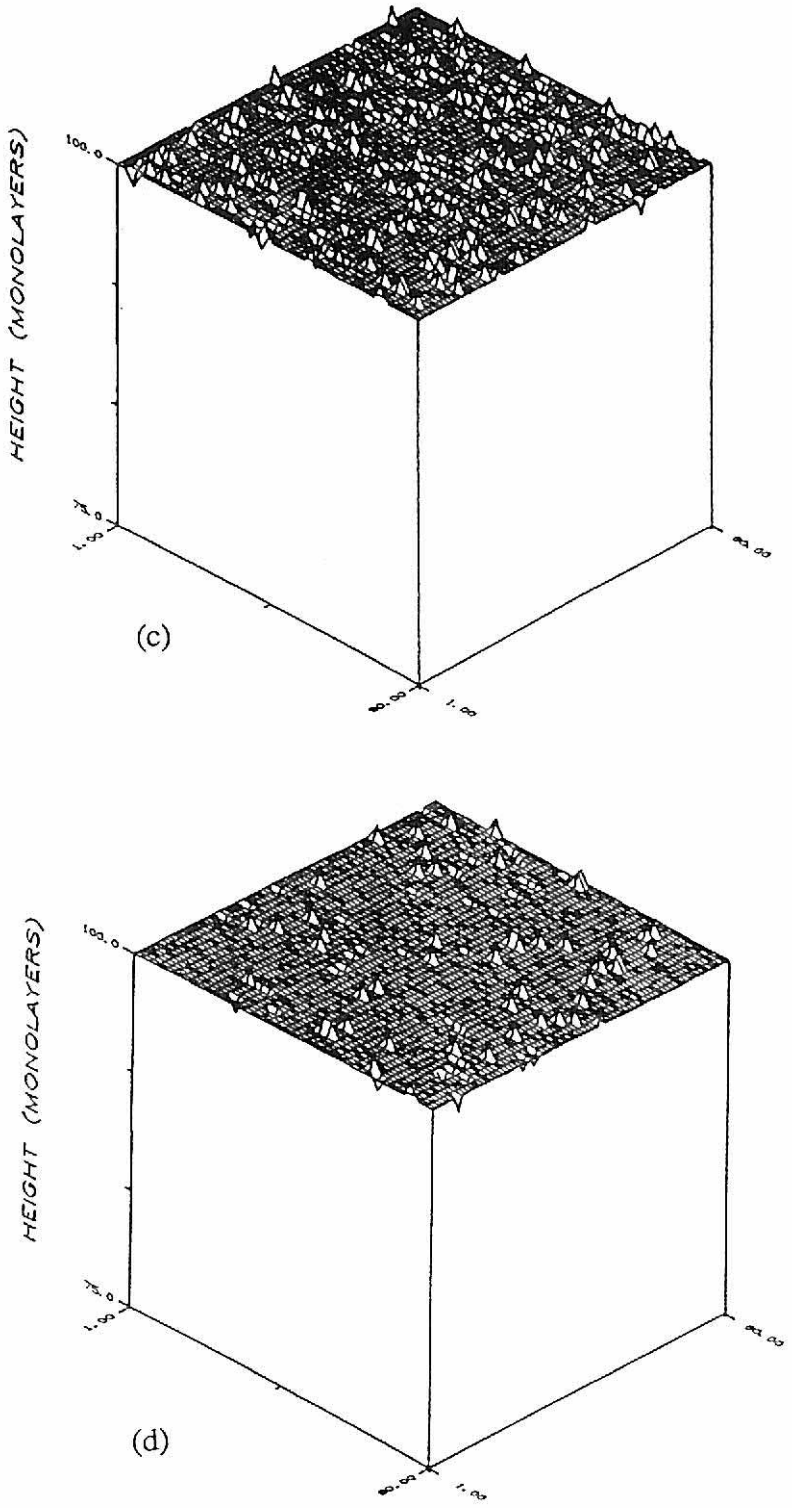

Figure III-14, continued. Stack heights vs wafer position for growth on an initially smooth surface with P_r varied for (c) $P_r=10^{-2}$ and (d) $P_r=10^{-3}$.

REFERENCES

[1] B. L. Chin and E. P. van de Ven, Solid State Technol. **31**, 119 (1988).

[2] A. C. Adams, Solid State Technol. **26**, 135 (1983).

[3] S. Rojas, A Modelli, and W. S. Wu, J. Vac. Sci. Tech. B **8** (6), 1177 (1990).

[4] A. J. Learn, J. Vac. Sci. Technol. B **4** (3), 774 (1986).

[5] R. M. Levin and K. Evans-Lutterodt, J Vac. Sci. Technol. B **1** (1), 54 (1983).

[6] K. Law, J. Wong, C. Leung, J Olsen, and D. Wang, Solid State Technol. **32**, 60 (1989).

[7] F. S. Becker, D. Pawlik, H Azinger, and A. Spitzer, J. Vac. Sci. Technol. B **5** (6), 1555 (1987).

[8] J. C. Schumacher Co.,Newsletter N. **32**, (1986).

[9] S. Nguyen, D. Dobuzinsky, D. Harmon, R. Gleason, and S Fridman, J. Electrochem. Soc. **77** (7),2209 (1990).

[10] C. P. Chang, C. S. Pai, and J. J. Hsieh, J. Appl. Phys. **67** (4), 2119 (1990).

[11] L. L. Tedder, Guangquan Lu, and J. E. Crowell, J. Appl. Phys. **69** (10), 7037 (1991).

[12] C. S. Pai and C.-P. Chang, J. Appl. Phys. **68** (2), 793 (1990).

[13] N. Selamoglu, J. A. Mucha, D. E. Ibbotson, and D. L. Flamm, J. Vac. Sci. Technol. B **7** (6), 1345 (1989).

[14] S. R. Kalidindi and S. B. Desu, J. Electrochem. Soc. **137** (2), 624 (1990).

[15] G. B. Raupp and T. S. Cale, Chemistry of Materials **1** (2), 207 (1989).

[16] M. Ikegawa and J. Kobayashi, J. Electrochem. Soc. **136** (10), 2982 (1989).

[17] M. J. Cooke and G. Harris, J. Vac. Sci. Technol. A **7** (6), 3217 (1989).

[18] S. P. Mukherjee and P. E. Evans, Thin Solid Films **14**, 105 (1972).

[19] Seshu B. Desu, J. Am. Ceram. Soc. **72** (9), 1615 (1989).

[20] C. Pavelescu and I. Kleps, Thin Solid Films **190**, L1-L3 (1990).

[21] A. M Nguyen and S. P. Murarka, J. Vac. Sci. Technol. B **8** (3), 533 (1990).

[22] D. Pramanik, Semicond. Int. **11**, 94 (1988).

[23] N. Lifshitz, G. Smolinsky, and J. M. Andrews, J. Electrochem. Soc. **136** (5), 1440 (1989).

[24] G. B. Raupp and T. S. Cale, J. Vac. Sci. Tech. B, to be published.

25 J. J. Hsieh, D. E. Ibbotson, J. A. Mucha, and D. L. Flamm, Mat. Res. Soc. Symp. Proc. **165**, 107 (1990).

26 D. E. Ibbotson, J. J. Hsieh, D. L. Flamm, and J. A. Mucha, SPIE Monitoring and Control of Plasma-Enhanced Processing of Semiconductors **1037**, 130 (1988).